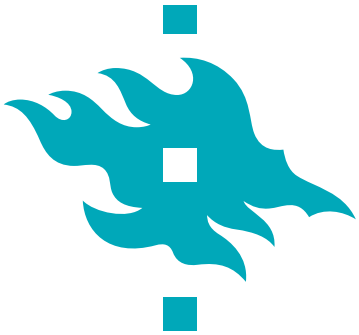

DISSERTATIONES SCHOLAE DOCTORALIS AD SANITATEM INVESTIGANDAM
UNIVERSITATIS HELSINKIENSIS

DUNJA NOVAKOVIC

SUPERFICIAL INTERACTIONS: THE IMPORTANCE OF SURFACES IN THE CRYSTALLIZATION, STABILIZATION AND DISSOLUTION OF AMORPHOUS DRUGS

DIVISION OF PHARMACEUTICAL CHEMISTRY AND TECHNOLOGY
FACULTY OF PHARMACY
DOCTORAL PROGRAMME IN DRUG RESEARCH
UNIVERSITY OF HELSINKI

Division of Pharmaceutical Chemistry and Technology
Faculty of Pharmacy
University of Helsinki
Finland

Superficial interactions: the importance of surfaces in the crystallization, stabilization and dissolution of amorphous drugs

by

Dunja Novakovic

ACADEMIC DISSERTATION

To be presented, with the permission of the Faculty of Pharmacy of the University of Helsinki, for public examination in lecture room Athena 302, Siltavuorenpenger 3 A, on 10th January 2020, at 12 noon.
Helsinki, September 2019

Supervisors Associate Professor Clare J. Strachan
Division of Pharmaceutical Chemistry and Technology
Faculty of Pharmacy
University of Helsinki
Finland

Professor Timo Laaksonen
Faculty of Engineering and Natural Sciences
Tampere University
Finland

Docent Leena Peltonen
Division of Pharmaceutical Chemistry and Technology
Faculty of Pharmacy
University of Helsinki
Finland

Dr Antti Isomäki
Biomedicum Imaging Unit
Faculty of Medicine
University of Helsinki
Finland

Dr Sara Miller
Research Fellow
Department of Chemistry
University of Otago
New Zealand

Reviewers Senior Scientist Kirsten Gräser
Pharmaceutical Preformulation - Pre-Clinical CMC
Roche Pharma Research and Early Development
Hoffmann La Roche
Switzerland

Senior Research Fellow Cushla McGoverin
Department of Physics
University of Auckland
New Zealand

Opponent Associate Professor Lidia Tajber
School of Pharmacy and Pharmaceutical Sciences
Trinity College Dublin
Ireland

ISBN 978-951-51-5738-6 (paperback)
ISBN 978-951-51-5739-3 (PDF)
ISSN 2342-3161 (print)
ISSN 2342-317X (online)

Hansaprint Oy, Helsinki 2019

Abstract

Active pharmaceutical ingredients can assume a diverse spectrum of solid-state forms. These forms differ in properties that are of utmost importance for pharmaceutical performance, such as solubility, dissolution rate and bioavailability. Thus, selection of a suitable solid-state form is highly important, particularly for the growing number of poorly water-soluble drug molecules. The amorphous (i.e. non-crystalline) form offers an often much needed solubility advantage at the price of thermodynamic physical instability and possible recrystallization. As the number of poorly water-soluble molecules in drug development is growing, so is the interest in the amorphous form and strategies for its stabilization. Formation of amorphous polymeric solid dispersions is the most common answer. However, issues with recrystallization, particularly at the surface, still remain, as well as high polymeric loadings.

The importance of differentiating between the surface and bulk properties of pharmaceutical materials is becoming increasingly recognized. Processes such as dissolution or chemical reactions with surrounding materials start from surfaces. For drugs in the amorphous form, inevitable recrystallization starts at the surface. This transformed (partly) crystalline surface thus dictates dissolution (or lack thereof), as well as other properties relevant for manufacturing, shelf-life or administration. This is why understanding, monitoring and manipulating superficial phenomena is of such importance.

Most established solid-state analytical methods show no or limited surface specificity. Nonlinear imaging (sum frequency generation (SFG) and coherent anti-Stokes Raman scattering (CARS)) are relatively new solid-state and surface specific methods. Moreover, as imaging methods, they can visualize solid-state distribution at the surface. Therefore, this thesis utilized novel nonlinear imaging approaches to better understand surface solid-state behavior. Further, the importance of surfaces in the crystallization, stabilization and dissolution of amorphous drugs was investigated.

The first part of the thesis established surface and solid-state specific non-linear imaging methods capable of distinguishing multiple solid state forms. SFG imaging proved to be an excellent tool in detecting low levels of surface crystallization (undetectable with other analytical methods employed), in particular amorphous transformation to a single crystalline solid-state form. Additionally, multimodal nonlinear imaging (SFG and CARS modalities, each with their own benefits) was used for the first time in pharmaceutical samples to simultaneously differentiate up to three different solid-state forms.

The second part of the thesis compared surface versus bulk crystallization and investigated surface crystallization (change in the solid-state form) during storage, as one of the key indicators of pharmaceutical performance. Both the cross-sectional SFG imaging of compressed powders, as well as the SEM morphology of continuous particle tablets allowed visualization of the surface-biased crystallization during storage. Further, the addition of different excipients physically mixed with the drug affected the crystallization of the amorphous drug in the bulk, however, their inability to stabilize the crystallization at the surface was demonstrated. In contrast, thin polymer coatings were successful in delaying the onset of surface crystallization at high humidity and elevated temperature during storage.

The final part of the thesis investigated the implications of storage-induced surface crystallization and its stabilization with polymer coatings on pharmaceutical performance during dissolution, as a further necessary step in drug development. It was shown that different extents and natures of surface crystallinity affect drug dissolution. Multimodal nonlinear imaging revealed up to five solid-state forms simultaneously present at the surface, and aided the interpretation of the dissolution profiles. The initial dissolution rates of the short-term stored polymer coated samples were equivalent to those of the unaged uncoated samples.

In summary, this thesis demonstrated the importance of surface solid-state properties, and their surface-specific analysis, for understanding the pharmaceutical performance of amorphous formulations during storage and dissolution. With further developments in amorphous drug formulations, the interest in surface crystallization and its prevention in the future will likely increase, together with the demand for surface-specific solid-state analysis. Altogether, it can be expected that in the future the understanding and utilization of surface phenomena will evolve from superficial to comprehensive.

Acknowledgements

This work was carried out at the Division of Pharmaceutical Chemistry and Technology at the Faculty of Pharmacy, University of Helsinki, Finland. Many of the experiments were performed at the Biomedicum Imaging Unit at the Faculty of Medicine, University of Helsinki, Finland. Part of the work was carried out at the Technical University of Denmark (DTU Health Tech) and the Department of Pharmacy at the University of Copenhagen, Denmark. The Doctoral Programme in Drug Research (DPDR) at the University of Helsinki and Center for International Mobility (CIMO) are gratefully acknowledged for funding that made this work possible.

I would like to thank all my five PhD thesis supervisors for asking me questions and making me learn and make conclusions on my own, rather than providing me with ready-made answers. My main supervisor, Assoc. Prof. Clare Strachan is deeply thanked for having trust in me, for giving me encouragement and nudge in the right direction, for openly sharing her network, passion for science, world of solid-state analysis and spectroscopy and for being the ultimate perseverance role model. Prof. Timo Laaksonen and Dr. Leena Peltonen are thanked for their patience and scientific input during our numerous long meetings and their generally positive "let's submit" attitude. Dr. Antti Isomäki is thanked for picking up my calls late in the evening when the tablet fell into objective revolver of a very pricey CARS microscope. On a more serious note, for always prompt feedback and all nonlinear optics related help. Dr. Sara Fraser-Miller, thank you especially for your occasional encouraging messages not related to my experiments or results.

I had dreams of my own PhD journey before starting it, but it was the strength of Darko's and Ruzica's support, which made me believe anything is possible, even when I doubted myself.

My follow up group committee members, Ass. Prof. Karin Kogermann and Prof. Jyrki Heinämäki from the University of Tartu, Estonia, are thanked for their encouragement and positive attitude towards my work. I wish to deeply thank all my co-authors. Jukka, thank you for making the time in the cold and dark room with lasers run faster and for always being positive and saying "it looks good" in the lab. May, thank you for our successful collaboration even with just email and Skype correspondence. Ass. Prof. Line Hagner Nielsen is thanked for inviting me to her research group and for always having time to catch up and listen.

I would like to thank all members of the Division of Pharmaceutical Chemistry and Technology, especially all Formulation and Industrial Pharmacy (FIP) group members. Flavia, Sara, Markus and Jaana Hautala, thanks for being friendly and welcoming especially in my first weeks and months in Helsinki. Sanna, thank you for your (highly skilled) help with experiments and trusting me with your special pipette during my last weeks in the lab prior to thesis writing. Heikki, thank you for technical assistance in various aspects and with many instruments at the lab. All members of FIP lunch group are thanked for taking my mind off work during our lunch breaks. Mikael, thank you also for giving me unexpected "nice to see you" hugs after not seeing me for a while. All Erasmus (BSc and MSc) students that I supervised (Pia, Marta, Bibi and Katarina), I hope you learned something from me as I have certainly learned from you.

I wish to thank my Powder Ranger Girls, Jaana, Jenni, Emmi and Tiina, and yet another unofficial Powder girl Sofia for giving me a sense of belonging. Sorry that it took me a while. Thank you all for yoga classes, Kallio neighborhood fun, cherry blossom and Rhododendron park moments, all the fun in San Diego, make-your-own-sushi nights and stress-less tote bag painting on a sunny pavement. Jenni, thank you for being a friend and both powder and power girl and thus making me feel positive towards after-PhD-thesis life. Jaana, thank you for being a true peer support and friend, for listening, for sharing and caring, and for lending me #Ronjathedog and her warm snout support.

My outside-of-work friends and family are thanked for all their support and understanding, and my parents in particular, for finding the strength to let me pursue my own dreams. Darko, thank you for holding my hand when I needed it and for understanding how difficult this all was at times. Helsinki, thank you for being undazzling and unpretentious but simply wonderful.

I feel that these four years weren't enough. There are still many cool experiments left undone, many smart and dear people that I didn't get to spend enough time with. This journey would not have been possible without all the people and places listed above (and many others not specifically mentioned), however, it was, particularly at certain times, a rather solitary experience that demanded grit and resilience while simultaneously taking care of other aspects in life. It was far from easy, but I made it. And it feels good to be on the other side.

Contents

Contents

List of original publications

This thesis is based on the following publications:

I Mah PT, **Novakovic D***, Saarinen J*, Van Landeghem S, Peltonen L, Laaksonen T, Isomaki A, Strachan CJ. Elucidation of compression-induced surface crystallization in amorphous tablets using sum frequency generation (SFG) microscopy. *Pharmaceutical Research* 2017; 34(5): 957-970.

II **Novakovic D***, Saarinen J*, Rojalin, T, Antikainen O, Fraser-Miller SJ, Laaksonen T, Peltonen L, Isomäki A, Strachan CJ. Multimodal nonlinear optical imaging for sensitive detection of multiple pharmaceutical solid-state forms and surface transformations. *Analytical Chemistry* 2017; 89(21): 11460-11467.

III **Novakovic D**, Isomäki A, Pleunis B, Fraser-Miller SJ, Peltonen L, Laaksonen T, Strachan, CJ. Understanding dissolution and crystallization with imaging: A surface point of view. *Molecular Pharmaceutics* 2018; 15(11): 5361–5373.

IV **Novakovic D**, Peltonen L, Isomäki A, Fraser-Miller SJ, Nielsen LH, Laaksonen T, Strachan, CJ. Surface stabilization and dissolution rate improvement of amorphous compacts with thin polymer coatings – can we have it all? *Submitted.*

The publications are referred to in the text by their roman numerals (**I-IV**). In publications I and II, the second two and the first two authors, respectively, contributed to the publication equally (*).

Additional publication

Additional publication, which is not included in the experimental part of this thesis, is listed below:

1. Mah PT, Peltonen L, **Novakovic D**, Rades T, Strachan CJ, Laaksonen T. The effect of surfactants on the dissolution behavior of amorphous formulations. *European Journal of Pharmaceutics and Biopharmaceutics* 2016; 103: 13–22.

Abbreviations and symbols

2D	two-dimensional
3D	three-dimensional
API	active pharmaceutical ingredient
ATR	attenuated total reflectance
BCS	Biopharmaceutics Classification System
CARS	coherent anti-Stokes Raman scattering
CMA	critical material attributes
CPP	critical process parameters
CQA	critical quality attribute
DMA	dynamic mechanical analysis
DSC	differential scanning calorimetry
(FT)IR	(Fourier-transform) infrared spectroscopy
GIT	gastrointestinal tract
HPMC(AS)	hydroxypropyl methylcellulose acetate succinate
ICH	International Conference on Harmonization
IDR ($mg/cm^2/s$)	intrinsic dissolution rate
NA	numerical aperture
M_w	molecular weight
PC(A)	principal component (analysis)
PEG	polyethylene glycol
PLM	polarized light microscopy
PVP	polyvinylpyrrolidone
QbD	quality by design
RH	relative humidity
SD	amorphous solid dispersion
SEM	scanning electron microscopy
SFG	sum frequency generation
SHG	second harmonic generation
SRS	stimulated Raman scattering
ssNMR	solid-state nuclear magnetic resonance
TERS	tip-enhanced Raman scattering
T_g (°C)	glass transition temperature
T_K (°C)	Kauzmann temperature
T_m (°C)	melting temperaure
ToF-SIMS	time-of-flight secondary ion mass spectrometry
TPEF	two-photon excited fluorescence
TPI	terahertz pulsed imaging
XR(P)D	X-ray (powder) diffraction
Δk (cm^{-1})	wavenumber difference
λ (nm)	wavelength

1 Introduction

The number of drug candidates is continuously increasing, especially with modern computational design approaches to high throughput drug discovery. Active pharmaceutical ingredients (APIs) are administered not as pure substances, but within dosage forms or drug products. Oral dosage forms (such as tablets and capsules) are the most commonly used products, and are also favored by most patients. In the body, the API must dissolve, i.e. release from the dosage form into solution, in sufficiently high concentrations. Dissolved API can permeate the intestinal wall to reach the bloodstream and its pharmacological target. This is a problem for the APIs under development because they are increasingly poorly water-soluble. Thus, despite the good efficacy (activity against the target) and safety profiles, many synthetized molecules have issues in becoming drug candidates. This makes the solid-state form of a poorly water-soluble API potentially as important as its chemical structure. Namely, different solid-state forms of APIs (e.g. polymorphs, salts, solvates and the amorphous form) have different physicochemical properties. Most importantly, apparent solubility and dissolution rate of an API can be improved by the use of a different solid-state form.

The use of the amorphous form is especially attractive in this context. The amorphous form offers the highest solubility and dissolution rate advantage, albeit at a cost of thermodynamic and physical instability and a strong tendency towards crystallization. Thus, to utilize the full potential of APIs in the amorphous form, an understanding of its crystallization behavior, its detection at an early stage and its prevention during the product manufacturing and shelf life are needed. Moreover, the influence of crystallization both prior to and during exposure to aqueous environments (such as during administration) needs to be investigated. This is because the solid-state form (amorphous versus different crystalline forms) will affect pharmaceutical performance during manufacturing, storage and administration. For these reasons, analytical methods that enable detection of low levels of crystallinity are needed. Such analytical methods can aid understanding and in addition provide earlier insights during stability studies, which are often time consuming. In addition, new stabilization strategies for the amorphous drug form are needed in order to prevent drug development failures and associated costs.

This thesis focuses on the characterization and influence of the physical (solid-state) form of small molecule APIs on product performance. In particular, the solid-state form at the surface of dosage forms is investigated. This is achieved through *a)* development of an analytical approach for identification of multiple solid-state forms, *b)* comparison of surface versus bulk solid-state forms and their transformations during storage, and *c)* monitoring dissolution performance and solution-mediated phase transformations upon storage. The work specifically emphasizes the importance of characterizing and understanding solid-state forms and associated transitions at the surfaces of dosage forms and their implications on stability and dissolution performance.

2 Review of the literature

2.1 Solid-state forms of drugs and their transformations

One of the most important tasks in solid dosage form development is the selection of the optimal solid-state form of the API. One has to consider all the potential polymorphic forms, states of solvation, and the degree of crystallinity, as they all strongly influence the product performance. The vast majority of small-molecule pharmaceutical APIs exist in multiple solid-state forms (**Figure 1**), many of which, one can assume, are yet to be discovered.[1] High-throughput discovery of new chemical entities results in excellent target activity. However, these drug molecules are becoming larger with an increasing number of functional groups, which further increases the likelihood of different solid-state forms. Therefore, the solid state of both old and new APIs requires a careful consideration.

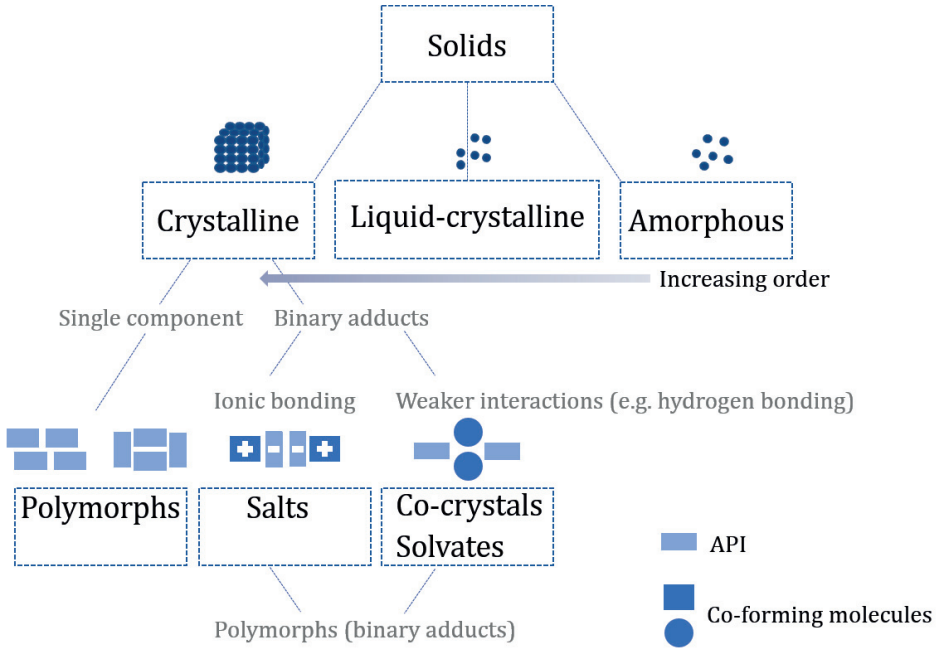

Figure 1 *A simplified representation of the diversity of solid-state forms, including single and two-component systems. In reality, ternary and quaternary systems also exist, as well as their polymorphs and salts (e.g. salt of a solvate).[2] Further, multicomponent systems can also be amorphous, and liquid-crystalline materials can be sub-divided into several structural classes.[3]*

Different solid-state forms of APIs have different physicochemical properties (such as solubility, dissolution, hygroscopicity, density and flowability, to name a few). Regulatory authorities require monitoring of solid-state forms. Generic companies can file marketing authorization applications with different solid-state forms of an already approved API, given

that the reference to safety and efficacy of a reference product can be made. Single marketing authorization can include different solid-state forms (such as hydrates and polymorphs) if their differences (e.g. in solubility) are not of clinical significance.[2] Importantly, solid-state forms can be patented. One form that has attracted a lot of attention in the last twenty years is the amorphous form. As high-throughput discovery often results in poorly water-soluble molecules,[4, 5] the use of an amorphous form, which can improve solubility, dissolution rate and finally bioavailability, is increasingly becoming of interest.[6] Moreover, it is crucial not only to properly select the physical form of the API, but also to understand any potential solid-state transformations that may occur during processing steps, storage or administration. Both the extent of these transformations and the properties of the transformed phase will ultimately govern the behavior and product performance. Thus, solid-state form identification, characterization and selection, as well as monitoring of potential solid-state transformations during the life of the drug are crucial for both product optimization and market exclusivity reasons.[7, 8]

2.1.1 Crystalline drug forms

The majority of dosage forms are formulated with API(s) in their thermodynamically stable, crystalline form. The term *solid state* form often implies a single chemical-component crystalline form, but it further includes multicomponent crystals such as solvates and hydrates, as well as the disordered amorphous form (**Figure 1**).[7] The crystalline form possesses a highly ordered three-dimensional (3D) long-range structure (*crystalline lattice*) composed of building blocks called *unit cells*.[9] The position and arrangement of the molecules within the unit cell is characteristic for each crystal lattice. *Polymorphism*, the existence of chemically identical but physically different crystalline solid-state forms occurs when molecules can arrange and pack themselves differently within the unit cell, or, when molecules at the lattice sites differ in their orientation or conformation. At a given temperature and pressure, one of the polymorphs is thermodynamically stable. The others are metastable, and will eventually transform to the stable form. However, this transformation may require considerable activation energy and might be very fast or very slow depending on the exact conditions. The transformation timeframe, along with chemical stability and microbiological aspects will determine the product's expiration date. The most common multicomponent crystalline APIs are solvates, including hydrates, which have solvent molecules as part of their crystal lattice (water is the solvent molecule in hydrates). Surprisingly, there are only seven unique unit cell dimensions called crystal systems. Crystal systems are classified according to the symmetry of the unit cell, which is described by the lengths of axes and the angles between them. The majority of APIs belong to (in increasing symmetry) triclinic, monoclinic or orthorhombic crystal systems. For example, the γ and α forms of indomethacin belong to the triclinic and monoclinic systems, respectively. These crystal systems further form 32 point groups (crystal classes) upon the application of symmetry operations with ten basic molecular symmetry elements, such as a center of symmetry. Once these, together with translation as a symmetry operation in 3D, are accounted for, crystals can form 230 different *space groups*.[9]

Analysis of crystalline APIs commonly includes diffraction, thermal and spectroscopic techniques, including X-ray (powder) diffraction (XR(P)D), differential scanning calorimetry (DSC), and infrared (IR) or Raman spectroscopy. XRPD directly probes spatial arrangement, while DSC reveals thermal properties, which are defined by the spatial arrangements of molecules, and thus gives an indirect confirmation of the crystal structure. An X-ray diffractogram provides a unique fingerprint for crystal form identification as each crystalline lattice interferes with X-rays differently resulting in a unique pattern of diffraction peaks. Distinct thermal properties, such as a melting point (T_m) can be further used to characterize the crystal form. Unlike XRPD, DSC can provide insights into solid-state stability, as it can detect any potential phase transitions that help to identify stable versus metastable polymorphs.[8] Crystalline solids exhibit sharp and mostly narrow bands when probed with vibrational spectroscopic techniques (IR and Raman). These bands arise from absorption of infrared light from a broad band source (IR) or inelastic scattering of light (Raman). Vibrational spectroscopy can identify different polymorphs based on the band shifts and appearance/disappearance of bands due to different molecular conformations and interactions with nearest neighbor molecules (*intermolecular interactions*) in different polymorphs. This is because intermolecular interactions may distort the probed *intramolecular* (within a molecule) bonds and their symmetry, as well as coupling (in-phase or out-of-phase) of intramolecular vibrations of multiple molecules present in the unit cell.[10]

2.1.2 Amorphous drug form

New drug candidates synthesized according to computational chemistry discoveries are often poorly water-soluble. In the Biopharmaceutics Classification System (BCS),[11] these APIs are classified as class II (having low solubility and high permeability) or class IV, if, in addition to poor solubility, they have impaired permeability. In the BCS, solubility is dose related and an API is considered soluble if the highest single dose can be dissolved in 250 ml of buffer within the physiological pH range at 37°C.[12] From a chemical point of view, an API with medium intestinal permeability (the average heterocycle) and common clinical potency needs a minimum aqueous solubility of around 50 µg/ml.[4] There are multiple approaches to improve the solubility of these compounds, such as through salt formation, particle size reduction (nanocrystals) or formation of self-emulsifying or lipid-based systems. The selected approach will largely depend on whether the API is soluble in lipids ("grease-ball molecules"), or poorly soluble in almost all solvents ("brick-dust molecules"). For the latter, the use of metastable polymorphs offers a limited, but often insufficient, solubility advantage. One of the most attractive strategies in this context is the utilization of the amorphous, i.e. non-crystalline, drug form. The change from an ordered to disordered physical form leads to some interesting differences. For example, while the sugar cubes (crystalline sugar) and candy floss (amorphous sugar) are both sweet, dissolving a sugar cube in a cup of tea typically requires stirring, while the candy floss appears to melt (actually dissolves) in the mouth almost immediately.[8] This demonstrates in practice the amorphous form benefits of higher apparent solubility[13, 14] and faster dissolution (release into solution), when compared to its crystalline counterparts.[14]

In contrast to crystals, amorphous materials have a disordered molecular arrangement with no long-range order. However, short-range order between the neighboring molecules may be present. For instance, carboxylic acid or amide groups of molecules in the amorphous form may participate in hydrogen bonding. There is evidence for formation of dimers between indomethacin molecules in the quench cooled amorphous form.[15] Further, amorphous materials may have regions with different density and relaxation behavior creating a distinct microstructure.[16]

One of the typical methods to obtain the amorphous form in the laboratory is by quench cooling a melted crystalline material (**Figure 2**). If the cooling rate is sufficiently high, the molecules do not have enough time to orientate and arrange themselves into a structure with long-range order, and the recrystallization temperature (T_m) can thus be overrun. The molecules then form a supercooled liquid (*rubbery state*), and, with further cooling, the *molecular mobility* (movements of molecules) slows down and viscosity increases due to a decrease in the kinetic energy of the molecules. At a particular temperature, called the *glass transition temperature* (T_g), or more precisely the T_g α, molecular motions fall out-of-equilibrium with the cooling rate and the molecules become kinetically trapped in a *glassy (amorphous) state*. The transition from the rubbery to glassy state at T_g is characterized by an abrupt change in thermodynamic properties (enthalpy, volume and entropy) and viscosity, macroscopically visible as a change from very viscous liquid to a solid referred as a "frozen liquid". Hypothetically, if this transition would be absent, the material would further cool to the Kauzmann temperature (T_K) where its thermodynamic properties would be equal to those of the thermodynamically stable crystalline form, which ironically would not be beneficial for increasing the solubility and dissolution rate. It is worthwhile to note that different cooling rates, as well as other preparation methods, will generate different amorphous forms (depicted as *Glass 1* and *Glass 2* in **Figure 2**),[16, 17] characterized by different levels of dissolution improvement.[18]

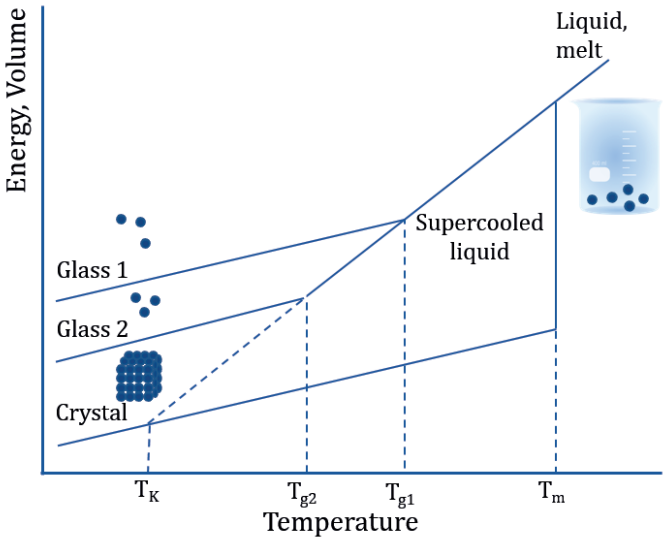

Figure 2 *The thermodynamic relationship of a crystalline and two amorphous solid forms as a function of temperature: melting temperature (T_m), glass transition temperature (T_{g1} and T_{g2}), and Kauzmann temperature (T_K). Glasses 1 and 2 are formed by fast and slow cooling rates, respectively. Modified from* [19].

The higher solubility of the amorphous form is due to its thermodynamic properties (especially higher energy in **Figure 2**) in comparison to the starting crystalline material. This can also be explained by the absence of a crystalline lattice that needs to be disrupted before the crystals can be dissolved and the molecules solvated. The improvements in solubility (10-1600 fold)[14] can ultimately enable the higher bioavailability of poorly water-soluble APIs.[6, 20]

One of the main thermal characteristics of an amorphous material is the presence of a T_g (T_g α), which is a second-order transition (as opposed to first-order transition, such as melting of a crystalline material), manifested as a heat capacity change, and consequently a baseline step change in a DSC thermogram. As opposed to the T_m, a glass transition is a kinetic event and the exact temperature, or more precisely average temperature and the temperature range, depends on the heating (or cooling) scan rate and the material's thermal history. This means that the observed T_g can change depending on how it is measured. T_g is typically used as one of the main parameters to describe the amorphous form and is usually measured with DSC, although it can also be measured by other techniques, e.g. dynamic mechanical analysis (DMA) and terahertz spectroscopy. The latter two methods can, in addition, differentiate between T_g α (global mobility or α relaxation) and T_g β (local mobility or β relaxation), which occurs prior to global (cooperative) motions that include surrounding molecules.[21]

As there is no defined structure, an XR(P)D diffractogram of an amorphous material will feature a broad pattern known as a halo, in which one or more very broad maxima, are present. The shape of the halo is a function of the average interatomic (and by extension intermolecular) distances in the amorphous solid. Vibrational spectroscopic techniques (IR and Raman) typically identify amorphous solids by band broadening, shifting and overlapping of bands present from their crystalline counterparts.[22] This is because the amorphous molecules form varying conformations and interactions with their nearest neighbor molecules (i.e. different bond angles and lengths), which results in a larger number of states with slightly varying vibrations.[23]

2.1.3 Crystallization

Being the highest energy and an unstable solid-state form, amorphous materials have a thermodynamic tendency towards crystallization.[6, 20] As opposed to *metastable* polymorphs, which are in a local free energy minimum of a potential energy surface, and can return to this minimum after a small displacement, *unstable* amorphous form can be visualized as a ball being on top or on the side of a free energy maximum, and even a small displacement can "push" the ball down the hill, where it will eventually stop at a local energy minimum (convert to a metastable polymorph) or global energy minimum (convert to a *stable* polymorph).

As opposed to crystalline forms where only molecular vibrations are present, all three modes of molecular mobility (vibrational, rotational and translational) are permissible in the amorphous state.[8] Thus, with time, molecules can change their arrangement, first by *relaxation*[24] (in which enthalpy is decreased[19] and increased molecular mobility leads to restructuring and e.g. formation of short-range order), and finally by *recrystallization* (formation of long-range order), including nucleation and crystal growth. This is the biggest hurdle in developing amorphous-based drug products.[25] If the crystallization is allowed to proceed, it will lead to the formulation reverting back to its starting poorly water-soluble crystalline state.

Therefore, detecting early-stage crystallization of an API and understanding its triggers (e.g. compression or exposure to aqueous environment) allows more efficient and reliable amorphous product development. As an added complexity, the crystallization of the amorphous form can result in different polymorphs, and even mixtures, depending on the conditions of crystallization. The ability to differentiate between these different solid-state forms in such cases becomes highly important, as they will dictate the product properties and pharmaceutical performance, e.g. dissolution, flowability and compactibility.

In a pharmaceutical setting, crystallization can occur in many steps. Solid-state transformations in the opposite direction – from a crystalline to the amorphous form – are also common during processing operations such as compression[26] and milling,[27] which mechanically introduce material disorder, and spray-drying, in which the transition occurs via a solution. Crystallization is thermodynamically driven and eventually inevitable, but its kinetics depend on environmental conditions (including exposure to heat, humidity[28], or pressure) during processing steps (such as compression),[29, 30] storage[31] and administration. Additionally, the presence of different excipients can affect the propensity for crystallization

of an API. Polyethylene glycol (PEG) is often found to promote crystallization, for instance in cryomilled mixtures with a single T_g[32, 33] although there are also studies in which it has been found to inhibit crystallization, for instance when used both within a two-component solid dispersion and an additional coating layer.[34] Low concentrations of PVP (1% w/w)[35] molecularly dispersed with indomethacin have been found to be protective against crystallization of amorphous drug.[36] In practice, amorphous formulations virtually always involve molecular level mixtures. In any event, a key prerequisite for further formulation development is a thorough understanding the crystallization behavior of the API itself.

2.2 Surface crystallization

Crystallization at the surface of an amorphous particle, film or tablet (**Figure 3**) is distinct from that of the bulk. It generally emerges earlier than crystallization in the bulk, [35, 37-39] with crystal growth often being orders of magnitude faster.[37-44] The reason for this difference is the higher mobility of molecules at the surface than in the bulk.[25, 45] There are multiple experimental findings that are suggestive of higher molecular mobility at the surface compared to the bulk. Firstly, crystals can grow tens to hundreds of nanometers upwards, away from the amorphous surface and toward the free space despite the increase in volume and surface area of the solid.[46, 47] Secondly, crystals at the surface are surrounded by depletion zones which widen and deepen over time.[43, 48] Thirdly, surface diffusivity (viscous flow) is orders of magnitude faster than bulk diffusivity and can sustain the fast growth of surface crystals.[49-51] This mechanism is responsible for the surface gratings becoming smoother over time.[49-51] Lastly, thin coatings made from different materials can inhibit or delay the surface crystallization by lowering the surface mobility to that of the bulk.[52-55] In fact, the suggested mechanism of bulk crystallization also involves surface mobility in the constantly created voids and new free surfaces introduced by crystal growth itself.[43, 56] This phenomenon also explains the two-stage kinetics of crystallization of amorphous solids – rapid initial surface crystallization followed by the slower crystallization in the bulk.[35, 37, 38]

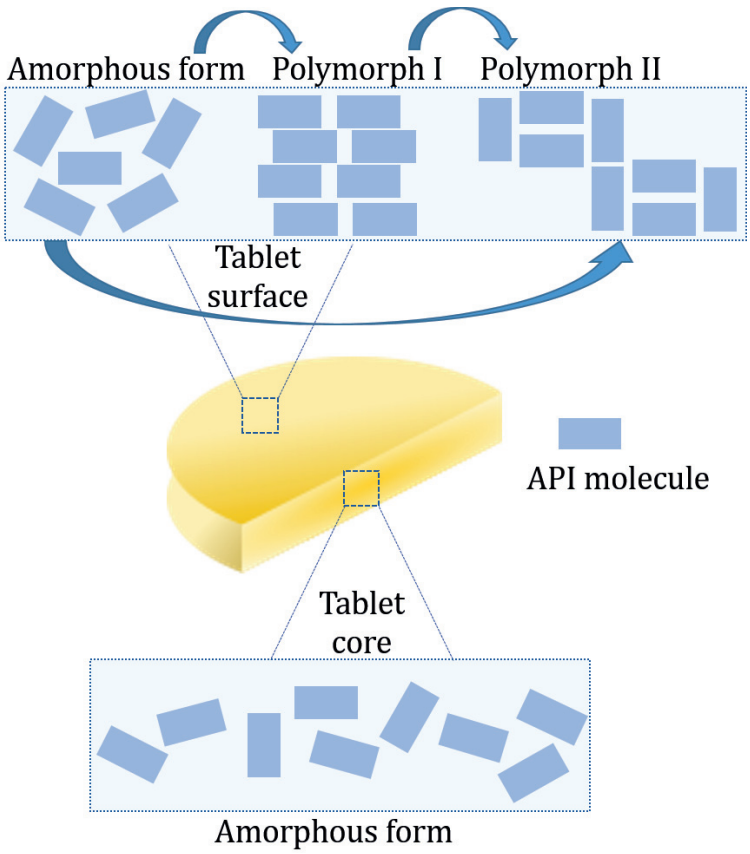

Figure 3 *Schematic representation of surface crystallization in an amorphous tablet. While the core of the tablet remains amorphous, the tablet surface (partly) transforms and crystallizes to one or multiple polymorphs, which can themselves transform to another (more stable) polymorph.*

Surfaces account for a small portion (weight fraction) of drug particles or dosage forms; however, their properties can disproportionately govern the behavior of the drug product as a whole. This is because pharmaceutically important physical transformations such as crystallization and dissolution start at the surface of solids. This is also why the surface specific analysis of the pharmaceutical materials and dosage forms is highly important and can provide insights unavailable with the techniques that probe the bulk, in which case the signal from the bulk dwarfs that from the surface.

2.3 Physical stabilization of the amorphous drug form

2.3.1 Solid dispersions

There are different approaches to stabilizing the amorphous drug form. Macromolecules such as *polymers* can be inhibitors of crystallization. Antifreeze proteins in arctic plants and fish prevent crystallization of water (ice formation) in extremely cold temperatures. In pharmaceutics, the use of polymers (such as polyvinylpyrrolidone (PVP) or hydroxypropyl methylcellulose (HPMC)) work in a similar manner. Instead of a liquid-to-solid phase change (such as the formation of ice), this section discusses prevention of solid-to-solid transformations by using pharmaceutical polymers. Multiple parameters affect the success of pharmaceutical polymer stabilizers: the polymer viscosity (affected by molecular weight (M_w) and potential branching and cross-linking), T_g of the polymer, hygroscopicity, miscibility of drug with the polymer, and potential drug-polymer interactions.

The most established strategy in stabilizing the amorphous drug form is the formation of *amorphous solid dispersions*[57] (SD) in which the drug is molecularly dispersed in the polymer matrix and forms a single phase with the dispersion characterized by a single T_g and an XR(P)D halo pattern.[58] In addition to the antiplasticizing effect of the polymer (characterized by an increase of the T_g above that of the drug alone),[28] and improved wetting due to the hydrophilic nature of many polymers, molecular level interactions such as hydrogen[59, 60] and particularly ionic bonding[61, 62] are very advantageous in inhibiting crystallization. Drug molecules in the SDs can be visualized as physically separated (molecularly dispersed) in between amorphous polymer chains in the matrix, such that the drug and polymer are intimately mixed.[63, 64] This reduces the molecular mobility (while increasing the T_g of the drug) and lowers the free energy of the system, as long as the drug loading is below the solubility limit. The formation of a SD is by far the most utilized approach in stabilizing the amorphous form, and its success is manifested as the presence of registered products on the market. Kaletra® tablets (lopinavir and ritonavir hot-melt-extruded with PVP/PVA (polyvinyl acetate)), Rezulin® tablets (troglitazone hot-melt-extruded with HPMC) and Sporanox® capsules (spray dried itraconazole with HPMC) are just a few examples of such marketed products.

Despite these successes, there is a disproportion between research output and the number of marketed products formulated as SDs. High polymer loadings can lead to high dosage volumes, which is undesirable. Further, the high hygroscopocity of some polymers and amorphous drug-polymer mixtures can cause chemical instability. Physical instability, with *phase separation* (formation of drug- and polymer-rich domains)[65] and consequent crystallization in particular, poses an issue. In this respect, SDs may be more efficient in stabilizing the bulk of the drug, while issues of surface crystallization may remain.[35, 47]

2.3.2 Other strategies in stabilizing the amorphous drug form

Alternative stabilization approaches include the formation of co-amorphous systems, in which the drug is combined with another small molecular species, such as an amino acid,

resulting in an amorphous molecular dispersion of the two compounds.[66, 67] Stabilization of co-amorphous systems is based on intimate mixing, complete miscibility of the two components, an increase in T_g (not as significant or high as for SD) and most importantly, molecular interactions which may include hydrogen bonding or salt formation.[64] Co-formers can alternatively be other materials, such as sugars, citric acid[68] or other APIs.[69] Sugars in nature, such as trehalose in mushrooms, prevent crystallization of water hydrating proteins (although this is rather a liquid-to-solid transformation). Stabilization by spatial confinement (volume restriction) can also prevent crystal growth. For example, confinement in pores (2-50 nm in size) of mesoporous silica/silicon[70-72] involves adsorption of drug molecules onto very large surface area of matrix of pores, which decreases the free energy. Spatial constraint prevents formation of clusters of molecules sufficiently large for nucleation.[71] Additionally, molecular interactions between the drug and silica matrix have been reported.[73] Finally, the amorphous form may alternatively be stabilized by complexation with macromolecules such as cyclodextrines.[58]

2.3.3 Thin (polymer) coatings

In contrast to dispersing the drug in a polymer matrix to form solid polymeric dispersions, applying a thin (polymer) coating layer can also stabilize the amorphous form, particularly at the particle, film or tablet surface, where other strategies may be less effective and stabilization is especially needed. This stabilization strategy is based on the hypothesis that in order to avoid crystallization, it is enough that only the surface is stabilized. The thin coating strategy has an additional benefit of lower polymer (or other stabilizer) burden, which leaves room for other potentially necessary excipients, a higher drug dose or allows for a smaller dosage form. Surprisingly little has been done using this approach, and **Table 1** contains an overview of such studies. The definition of thin coatings in these studies assumes coatings as thin as tens of nanometers deposited on the surface of amorphous drug films typically 5-50 μm in thickness. Additionally, individually dip-coated drug particles ("chunks" of amorphous glass), typically sieved to 45-100 μm are used.

Glass microscope coverslips [37] as well as a sputtered gold layers can lower the mobility of the superficial (or now interfacial) drug molecules to that of the bulk. These examples show that the interactions between the amorphous drug and the coating can be physical in nature (such as weak van der Waals interactions). On the other hand, strong ionic interactions between the drug and the coating material are very effective in stabilizing the amorphous drug against crystallization over time. For instance, better stabilization of chitosan,[74] in comparison to gelatin,[55] coatings of amorphous indomethacin could potentially be attributed to stronger chitosan-drug ionic interactions. Regardless of the nature of the interactions, thin surface coatings can significantly improve the stability of amorphous drugs. However, the lower physical stability of such coatings in humid storage conditions is noted.[74] Hence, the monitoring of critical quality attributes (CQA) at high humidity is especially important.[53]

Table 1 *Overview of selected publications in which the amorphous drug form is stabilized with thin coatings. Thickness, amount and/or size of API and coating is given where available.*

Authors	*Year*	*API*	*Coating*	*Deposition*	*Result/Conclusion*
Wu et al.[37]	2006	indomethacin films 15 µm	microscope slide	physical	removal of glass cover exposed amorphous interior
Wu et al.[52]	2007	indomethacin films 15 µm	gold 10 nm and polyelectrolytes (PDDA, PSS) 3-20 nm	sputtering, electrostatic	surface mobility lowered by coatings in nm range
Zhu et al.[40]	2008	nifedipine films 15 µm	gold 10 nm	vacuum	gold coating reduced surface crystallization to that of the bulk
Zhu et al.[38]	2010	grisefulvin films 15 µm	gold ~10 nm	sputtering	faster surface crystallization than previous APIs, suppressed by gold coating
Ng et al.[53]	2013	carbamazepine, celecoxib, felodipine, fenofibrate, films 5-10 µm	PVP K30, Eudragit E® PO, Soluplus®	spin coating	polymer coating more effective than SD
Priemel et al.[75]	2013	indomethacin particles 150-300 µm	Eudragit® E <37 µm or Soluplus® 150-300 µm particles	dry coating (mixing)	Eudragit® better stabilizer possibly due to higher surface coverage
Capece et al.[54]	2015	paracetamol, SD with PVP particles 15 µm	carnauba wax ~5 µm	dry coating (vibratory ball milling)	simultaneous milling and coating results in surface stabilization
Hsu et al.[34]	2015	naproxen-PEG SD	PEG	drop printing	higher M_w polymer better stabilizer
Teerakapib al et at.[55]	2018	indomethacin, nifedipine films 50 µm	gelatin 20 ±10 nm	dip-coating	no need for opposite charges of API and polymer
Zeng et al.[41]	2019	loratadine films 14 µm particles 70-80 µm	dextran 20 nm	dip-coating (electrostatic)	physical stabilization and increase in dissolution rate achieved
Gui et al.[42]	2019	clofazimine films 20 µm particles 45–100 µm	alginate several nm	dip-coating (electrostatic)	physical stabilization in elevated temperature and humidity up to one year
Li et al.[74]	2019	indomethacin particles 45–100 µm	chitosan several nm	dip-coating (electrostatic)	improved stability, dissolution, powder flow and tabletability

2.4 Analytical techniques in solid-state analysis

2.4.1 Established solid-state characterization methods

An array of techniques are available to choose from in modern solid-state analysis. They all have inherent advantages and disadvantages, with some of these highlighted for commonly used methods in **Table 2**. For instance, while XR(P)D is considered the gold standard in solid-state form identification, polarized light microscopy (PLM) is a simple, inexpensive and therefore commonly available tool to differentiate crystalline and amorphous systems. Vibrational spectroscopy (IR and Raman) provides both chemical (based on intramolecular vibrations) and solid-state (based on molecular conformation and intermolecular interactions) specificity. Both IR and Raman signals are based on a change in vibrational energy levels of molecules. The two techniques are complementary as their sensitivity to specific vibrational modes differs. While IR absorption is a function of the dipole moment change during a vibration, Raman scattering is a function of the polarizability change during the vibration. A potential disadvantage of conventional IR and Raman spectroscopies, is that low levels of certain physical forms (with different degrees of crystallinity or different polymorphic forms) may be difficult to detect. For instance, the spectra of different solid-state forms obtained with vibrational spectroscopy often exhibit subtle differences that are particularly hard to detect when solid-state forms are present in low quantities. Additionally, the listed techniques, with the exception of attenuated total reflectance (ATR) IR spectroscopy and microscopy, typically probe primarily the bulk of the material and the resulting measurements represent the averaged solid-state composition of the entire sample. As crystallization typically starts at surfaces, and can act as a catalyzing site for crystallization of the entire dosage form, there is a need for more suitable and sensitive methods to study surface crystallinity.

Table 2 *Overview of some widely-used solid-state analysis techniques and their advantages and disadvantages in commonly used set ups.*

Technique	*Benefits*	*Drawbacks*
Particular (assembly of molecules) level properties		
Diffraction-based		
XR(P)D	crystal form identification, quantification of crystallinity, non-destructive	limited surface specificity, preferred orientation effect
Thermal		
DSC	sensitive, quantification of crystallinity, small sample amount (~ µg)	limited surface specificity, destructive, difficult interpretation
Microscopy and electron microscopy techniques		
SEM	extremely high spatial resolution (~ 1 nm), small penetration depth	not directly solid-state specific
PLM	easy, inexpensive, sensitive to low levels of crystallinity	limited solid-state specificity, not suited to opaque solid dosage forms
Molecular level properties		
Spectroscopic (including microscopy) techniques		
Spontaneous Raman	signal intensity theoretically proportional to concentration, no sample preparation, can be used in aqueous systems	potentially weak signal, slow imaging, can be hindered by fluorescence, not always sufficiently surface specific
ATR-IR	relatively surface specific, no sample preparation	clamp pressure can induce crystallization, water interference
ssNMR	sensitive to low levels of crystallinity	slow analysis (hours), poor spatial resolution, not surface specific

2.4.2 Surface specific characterization methods

As this thesis focuses on surfaces, the following two chapters will introduce some surface specific characterization methods. This overview is however non-exhaustive.

Attenuated total reflectance (ATR) sampling in IR spectroscopy requires intimate contact between the sample and the ATR element (made of a high refractive index material such as diamond). Above a critical incident angle, incoming light reflects off the ATR element by total internal reflection, which generates an evanescent wave that penetrates into the sample. This method typically probes up to a couple of micrometers (100–300 nm up to 1–3 µm)[76] of the surface layer in contact with the element, which leads to the surface-specific sampling (the exact penetration depth depends on refractive index of the crystal and sample, angle of incidence and wavenumber). ATR spectroscopy (and microscopy) is the most surface-specific of all traditionally used solid-state analysis methods.[77]

In the analysis of multicomponent systems such as in pharmaceutics, imaging (spatially resolved) techniques have many benefits. Vibrational spectroscopic imaging (ATR and Raman) are both spectrally (providing chemical and solid-state specificity) and spatially

resolved. In other words, imaging methods generate *data hypercubes*, in which the spatial (*x* and *y*) dimensions are accompanied by the spectral (*z*) dimension.[76] In practice, spatial information means that individual spectra from specific regions of interest (pixels, i.e. picture elements) can be extracted, allowing for visualization of distribution patterns, for example in dissolution.[78] Lateral (*x*-*y*) spatial resolution on the order of 4 μm and 1 μm for ATR IR and Raman analyses, respectively, can be achieved (resolution is diffraction limited and thus is limited by the wavelength(s) of the light, in addition to depending on numerical aperture (NA) of the objective and wavelength).[76] Raman microscopy can provide an axial (also referred to as *z*) resolution of several micrometers (depth resolution is proportional to wavelength and inversely proportional to the objective $(NA)^2$). The confocal pinhole, depth probed and properties of the sample such as refractive index also effect the resolution obtained experimentally.[79] The advantages and disadvantages of spectroscopy and microscopy applications of these methods are listed in **Table 2**.

Some modifications to traditional XR(P)D enable higher surface specificity and depth profiling. In grazing (or glancing) incidence X-ray diffraction, the incident X-ray beam arrives at a small angle relative to the sample surface (typically < 5°). Knowledge of the incidence angle (and material density and M_w) allows the calculation of the X-ray penetration depth based on Parratt equation.[80] The penetration depth can be on the order of nanometers or micrometers. This method enables depth-profiling, for instance of dissolution[81] or compaction-induced[82] solid-state transformations.

Tip-enhanced Raman scattering (TERS) is highly surface-specific technique (axial resolution 1-100 nm),[83] which, in addition, offers a lateral resolution beyond the diffraction limit in the range of 10-20 nm. TERS combines Raman and atomic force microscopy (AFM)[84] and thus provides both chemical (and solid-state) specificity and surface topography information. Moreover, the local surface plasmon generation from the use of a tip in this Raman modification can enormously enhance the normally weak Raman scattering. However, this techniques is technically challenging, due to possible tip contamination, sample overheating and different degrees of Raman signal enhancement caused by topography effects.[83]

2.4.2.1 Analysis of (thin) coated systems

Important characteristics of thin-polymer coated systems described earlier are coating thickness and properties of the coated surface. Thus, this chapter introduces selected techniques which could be suitable for analysis of these properties, in addition to some earlier discussed methods (such as SEM, ATR IR spectroscopy etc.).

Terahertz pulsed imaging (TPI) involves the detection of terahertz pulse reflections off sample interfaces (including the sample surface), which occur due to refractive index changes. The reflections that occur below the surface are time delayed to that occurring at the surface.[85] This technique was developed and introduced for pharmaceutical analysis relatively recently to measure coating thickness, density and uniformity of coated tablets. Moreover, terahertz interface index can be used for probing the physicochemical properties at the interface between the coating and tablet core.[86] This technique is excellent for fast

and non-destructive imaging of coating thickness over whole tablets, however, it is generally limited to thicker coatings, typically above 35 μm.[85]

Time-of-flight secondary ion mass spectrometry (ToF-SIMS) is an example of a highly surface-specific analytical method (analysis depth ~1 nm) in which ionized atoms, molecules and molecular fragments from the sample surface are detected based on the transit time needed to reach the detector.[87] By measuring the time-of-flight, mass-to-charge ratios and mass spectra can be deduced. High surface specificity is both an advantage and disadvantage of this method. In static mode, ToF-SIMS is exclusive to the first monolayer of a sample, while in the depth profiling, penetration is typically limited to hundreds of nanometres.[88] Hence, such analysis can be complemented by confocal Raman microscopy that can probe deeper structures, albeit with a much lower axial resolution (several micrometers).[89]

The applications of multivariate analysis aided solid-state analysis with ToF-SIMS is in its infancy,[90] and it is generally recognized that the greatest disadvantage of mass spectrometry and ToF-SIMS is the inability to differentiate between compounds with the same molecular weight, which naturally extends to polymorphs. Similarly, TPI, as opposed to terahertz pulsed spectroscopy,[91] does not currently provide spectroscopic solid-state information.

2.4.3 Nonlinear optical imaging

Nonlinear optical imaging is a relatively novel analytical technique that provides surface and solid-state specific, spatially resolved information.[92, 93] Nonlinear optical phenomena result from multiphoton interactions (**Figure 4**). In second-order processes, two incident photons interact with the sample material, while the third-order processes three incident photons interact with the sample. As a result of the multiphoton interactions, a photon with a wavelength different than that of the incoming photons is generated.[93, 94] For efficient generation of nonlinear signals, both temporal (arrival at the same time) and spatial (same position within the sample) overlap of interacting photons are needed. The nonlinear signal is produced only in the focal volume, accounting for the intrinsically confocal nature of nonlinear phenomena (i.e. no pinhole is needed). This allows non-destructive plane-by-plane 3D optical sectioning, while at the same time reducing the background signal and photodamage.[95] The axial (depth) resolution of these methods is on the order of 0.9 μm[96] while the lateral resolution is diffraction limited and in the range of 300–500 nm.

The interaction of matter and light (electromagnetic wave) results in polarization (displacement of electron cloud) in the medium that generates a new electromagnetic field called polarization wave at the atomic/molecular level. Mathematically, polarization (***P***) can be described as a power series (**Equation 1**) with increasing order of nonlinearity, where ε_0 is the permittivity of free space and χ is the linear susceptibility.[94]

(1) $$P = P^{(0)} + \underbrace{\varepsilon_0 \chi^{(1)} \cdot E}_{P^{(1)}} + \underbrace{\varepsilon_0 \chi^{(2)} \cdot EE}_{P^{(2)}} + \underbrace{\varepsilon_0 \chi^{(3)} \cdot EEE}_{P^{(3)}} + \cdots$$

In linear processes (such as reflection and spontaneous Raman scattering), the incoming field strengths (***E***) are moderate and the resulting polarization is directly proportional to the incoming field of light. Thus, the generated polarization wave maintains the same frequency and wavelength as incident light. Nonlinear processes are possible only when the intensity of incident light (external electromagnetic field) is much higher compared to linear processes (~10^6 Vm^{-1}). In such cases, the higher order terms in **Equation 1** can no longer be neglected and the nonlinear response, as opposed to the linear response, is no longer directly proportional to the electromagnetic field of the light, meaning that new frequencies are generated.[92] In practice, introducing high energy fields involves the use of ultrashort (pico- or femtosecond) pulsed lasers which provide high peak powers.[95] The use of high NA objectives is also standard.[95]

In order to obtain a nonlinear signal, a so-called phase matching condition has to be fulfilled. This can be explained by the difference between the wavenumbers of the incident (ω) and generated (2ω) light waves (Δk) in **Figure 4**. Phase-matching and maximum intensity of the signal, occurs when wavenumber mismatch equals zero (waves start and stay in phase).[97] When Δk is not zero, the signal becomes increasingly out of phase (waves start, but do not stay, in phase) with increasing distance. Coherence length is the length in which waves can remain in phase. In practice, the short focal length of a high NA objective helps in achieving adequate phase matching within the focal volume where the nonlinear signal is generated.

There are several nonlinear imaging modalities that have been used in pharmaceutical research, including sum frequency generation (SFG), coherent anti-Stokes Raman scattering (CARS), stimulated Raman scattering (SRS) and two-photon excited fluorescence (TPEF). In context of this thesis, only the first two will be discussed in detail. *Multimodal* nonlinear imaging is when two (or more) nonlinear techniques are utilized simultaneously.

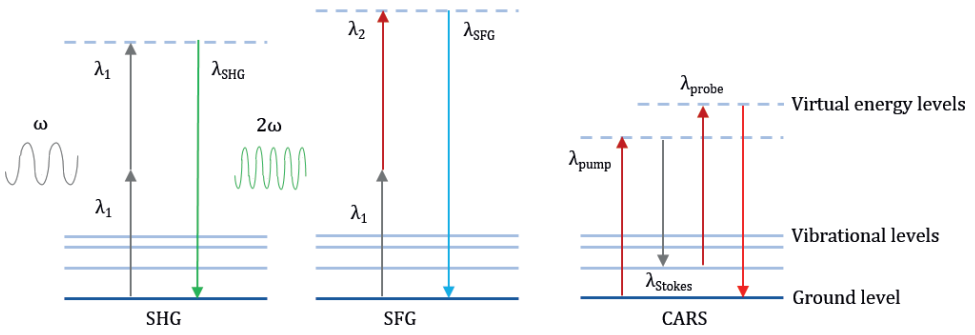

Figure 4 *Energy diagrams of SHG, SFG and CARS nonlinear processes. Each photon is represented as an arrow. Different colors of arrows indicate different wavelengths. Additionally, input and generated photons in SHG are shown as light waves with different frequency.*

2.4.3.1 Sum frequency generation (SFG)

SFG is a second-order nonlinear process which can occur only in samples lacking inversion symmetry. On a bulk level, this includes non-centrosymmetric crystals. Thus, SFG can differentiate non-centrosymmetric from centrosymmetric crystals and amorphous materials, which do not generate this signal. This is because the SFG signal is the sum of all interactions of all molecules in the sample. In isotropic systems (liquids, gases, and amorphous materials), where molecules are randomly oriented, the sum effect is a destructive interference and no SFG signal can be detected.[98, 99] SFG is especially suitable for detecting very low levels of crystallinity.[97-101] The best-known SFG-active biomedical substance is collagen, and in practice, many pharmaceutical crystals generate this signal as well.

As can be seen from the energy diagram (**Figure 4**), the incoming photons interact with each other in the sample and the generated photon has a frequency that is the sum of the frequencies of the two incident photons (hence the name). In wavelengths this can be expressed according to **Equation 2**, where λ_1 and λ_2 are incoming wavelengths, and λ_{SFG} is a generated wavelength.

(2) $$\lambda_{SFG} = \frac{1}{\frac{1}{\lambda_1}+\frac{1}{\lambda_2}}$$

Second harmonic generation (SHG) is a special case of SFG and the oldest demonstrated nonlinear optical signal, which was first observed in 1961.[102] In SHG, the two incoming photons have the same wavelength, and the resulting signal is at exactly half the wavelength (double the frequency) of the incident photons. Of the two, SHG is more frequently applied, as it requires only one laser source. Most commonly, SHG is used to create green light inside a widely available green laser pointers.

It is important to note that a symmetry break at an interface of either centro- or non-centrosymmetric materials, including amorphous materials, liquids and gases may also cause the appearance of SFG signal, however in such cases the signal is usually much weaker than any bulk generated SFG signal from non-centrosymmetric crystals, and depending on the experimental setup, may not be detectable.[92]

2.4.3.2 Coherent anti-Stokes Raman scattering (CARS)

As with spontaneous Raman spectroscopy, CARS is based on the detection of specific molecular vibrations. It requires an input of three photons and was first reported by Maker and Terhune at Ford Motor Company in 1965.[103] As can be seen from the energy diagram (**Figure 4**), the energy difference between the pump and Stokes photons is selected so that it matches a particular vibrational mode of the target molecule, in other words, a vibration of a chemical bond, such as C-H or carbonyl stretching. The targeted vibrational mode becomes enhanced and its resonant oscillation is then probed by the third photon, resulting in the generation of an anti-Stokes (shorter wavelength) photon. The relationship between

excitation wavelengths (λ_{pump} (nm) and λ_{Stokes} (nm)) and probed vibrational frequency ($\tilde{\nu}_{vib}$, expressed in wavenumbers (cm^{-1})) is given in **Equation 3**.

$$\tilde{\nu}_{vib} = \left(\frac{1}{\lambda_{pump}} - \frac{1}{\lambda_{Stokes}}\right) \times 10^7 \quad (3)$$

As all together four photons are involved, CARS is an example of four-wave mixing process. The pump and probe beams can originate from the same source, and thus at least two laser lines are necessary to generate the CARS signal. Altering the pump wavelength allows multiple vibrational resonances of the target molecule to be probed. Thus, and most importantly, CARS offers both chemical and solid-state selectivity.

Similar to conventional Raman microscopy, CARS imaging involves non-contact and non-destructive sampling, and does not require labels. Its main advantage over spontaneous-scattering Raman microscopy is orders of magnitude faster, video-rate imaging,[26, 104] higher spatial resolution,[96] and lack of single-photon fluorescence interference. Spontaneous Raman scattering is a rare phenomenon, occurring in only one in every 10^6-10^8 scattered photons. This explains why CARS, with the stimulated Raman effect is much faster. On the other hand, Raman microscopy typically provides higher spectral resolution and breadth, and consequently higher chemical specificity, which may be advantageous in the analysis of complex mixtures such as pharmaceutical formulations. Further developments in CARS instrumentation may overcome this limitation.[93] Disadvantages of CARS (and SFG) methods include potentially high peak laser powers (which may be damaging for sensitive samples), the nonlinear relationship of signal intensity to concentration and less widely assesible instrumentation.

2.4.3.3 Pharmaceutical applications

There is a growing interest in nonlinear imaging as an analytical approach in solid-state analysis of pharmaceutics, especially in the recent years.[93, 105-107] SHG has been applied for the analysis of crystallinity and polymorphism in pharmaceuticals for the first time by Strachan et al. in 2004.[97] CARS was used to image the distribution of lipids in emulsions in 2003.[108] Studies by Kang et al.[96, 109, 110] demonstrated the first applications of CARS in the area of solid dosage form analysis. An overview of some of the studies involving APIs, pharmaceutical excipients and dosage forms is given in **Table 3**.

Table 3 *Overview of selected publications utilizing nonlinear optics (including imaging) of drugs, excipients and dosage forms. Publications until year 2013 are modified from [111], while the rest are updated by the author.*

Authors	*Year*	*Method*	*Sample*	*Result/Conclusion*
Pautot et al.[108]	2003	CARS	Dodecane emulsions	CARS was capable of imaging variation in composition of emulsions

Strachan et al.[97]	2004	SHG	Enalapril maleate and PVP	SHG was very sensitive to trace levels of crystallinity in otherwise amorphous materials
Strachan et al.[112]	2004	SHG	Enalapril maleate, ranitidine, carbamazepine, lactose, PVP	SHG was used to measure polymorphism and crystallinity of various pharmaceutical materials
Kang et al.[96]	2006	CARS	Paclitaxel loaded polymer films	CARS microscopy was effective for imaging native drug molecules in polymer matrices
Kang et al.[109]	2007	CARS	Paclitaxel loaded polymer films	CARS microscopy showed that drug release from a polymer matrix is closely related with its distribution
Kang et al.[110]	2008	CARS	Paclitaxel loaded polymer films	CARS was useful in studying drug release from polymer films without drug labelling
Windbergs et al.[113] Jurna et al.[114]	2009	CARS	Theophylline containing tablets and lipid extrudates	CARS used to visualize the spatial distribution of different components in oral pharmaceutical dosage forms and drug release during dissolution
Slipchenko et al.	2010	SRS, CARS	Commercial Amlodipine tablets	SRS allowed selective imaging of drug molecules and excipients
Wanapun et al.[115]	2010	SHG	Amorphous griseofulvin and chlorpropamide	SHG was used to sensitively and selectively detect the existence and formation of crystalline APIs
Wanapun et al.[99]	2011	SHG	Amorphous griseofulvin	SHG allowed quantification of trace crystallinity (4 ppm) within bulk scattering powders
Toth et al.[116]	2012	TPEF, SHG	Griseofulvin, various excipients, commercial tadalafil tablet	Multiphoton techniques were explored for selective detection of model APIs in mixtures with common excipients
Kestur et al.[98]	2012	SHG	Naproxen-HPMCAS SD	SHG enabled sensitive quantification of the extent of crystalline material in drug-polymer SDs
Hsu et al.[117]	2013	SHG	Naproxen-PVP SD	SHG was used to analyze naproxen crystal growth at different temperatures
Garbacik et al.[118]	2013	CARS	Theophylline, mannitol, diprophylline and tristearin polymorphs	Hyperspectral CARS was capable of identifying multiple solid-state forms of the same compound
Fussell et al.[119]	2013	CARS	Theophylline anhydrate and monohydrate	*In situ* CARS microscopy of theophylline dissolution was correlated with polymorphic conversions with dissolution rate changes
Hartshorn et al.[26]	2013	CARS	Indomethacin in a simple tablet formulation	Two polymorphs and an amorphous form of indomethacin were distinguished
Zhu et al.[120]	2013	SHG	Naproxen/PEG SD	Interpretation of the influence of API domain size and distribution in a polymer matrix on dissolution performance was aided by SHG visualization

Chowdhury et al.[121]	2014	SHG	Amino acid (proline)	SHG confirmed crystallization of an amino acid through transient metastable forms according to Ostwald's rule of stages
Ghorab et al.[122]	2014	SHG	Maltodextrin and sucrose powder blends	SHG was used to monitor deliquescence and dissolution as a function of relative humidity
Pegoraro et al.[123]	2014	CARS, TPEF, SHG	Cellulose fibers and bulk bone	A multimodal imaging method comprised of CARS in the lower frequency regions, TPFE and SHG was developed and tested on bone and cellulose samples
Fussell et al.[124]	2014	CARS	Budesonide and salmeterol on lactose carriers	CARS microscopy was used to visualize the distribution of micronized drugs on coarse lactose carriers
Fussell et al.[70]	2014	CARS	Mesoporous silica particles loaded with itraconazole and griseofulvin	CARS enabled visualization of drug distribution and confirmed the amorphous nature of loaded drugs
DeWalt et al.[125]	2014	SHG	Naproxen	Crystal orientation effects were studied by polarization dependent nonlinear responses
Garbacik et al.[118]	2014	CARS	Diprophylline tablet	A three component thick tablet was imaged by epi-CARS
Jackson et al.[126]	2014	SHG	Danazol	SHG was used to detect the onset of crystallization from supersaturated solutions of danazol in presence or absence of polymers as crystallization inhibitors
Toth et al.[127]	2015	SHG, TPEF	18 different crystalline APIs	A computational model for predicting SHG activity of crystalline APIs was developed
Christophersen et al.[128]	2015	CARS	Solid lipid microparticles	CARS was used to image the distribution of lysozyme in solid lipid microparticles and aided evaluation of release profiles
Schmitt at el.[100]	2015	SHG	Commercial formulation of paclitaxel	SHG enabled detection of crystalline API in some batches of commercial amorphous *iv* formulations
Newman et al.[129]	2015	SHG	Ritonavir in HPMC matrix	SHG was used to guide synchrotron XRD analysis
Hsu et al.[34]	2015	SHG	Naproxen/PEG SD with PEG coating	Increased M_w of polymer coating retarded the moisture induced crystallization of API
Schmitt at el.[130]	2016	SHG	D-mannitol	Two polymorphs were discriminated within the 99.99% confidence interval in quantities typically available in high throughput polymorph screenings
Chowdhury et al.[131]	2017	SHG	Clopidogrel bisulphate	Two polymorphic forms of API in powder mixtures were discriminated
Correa-Soto et al.[132]	2017	SHG	Flutamide and ezetimibe SDs	Crystallization of SDs upon storage was detected earlier than with XRPD

Elkhabaz et al.[133]	2018	SHG	Ezetimibe SDs	SHG was used to monitor crystallization of SDs in biorelevant turbid dissolution media
Song et al.[101]	2018	SHG	Ritonavir SDs	SHG was used to monitor crystallization kinetics of SDs with 10 ppm as lower limit of detection
Ojarinta et al.[134]	2018	CARS, SFG	Ibuprofen/arginine and indomethacin/arginine co-amorphous mixtures	Multimodal nonlinear imaging showed distribution of components on the surface of simple tablet formulations
Porquez et al.[135]	2018	CARS	tablets with paracetamol, ibuprofen or cetirizine as APIs	Spectral focusing CARS was developed and used to distinguish APIs from excipients, including two paracetamol polymorphs in tablets
Smith et al.[136]	2018	SHG	Evacetrapib SDs in final dosage forms	An SHG method for quantification of crystallinity without a calibration curve was developed
Figueroa et al.[137]	2019	SRS	Pioglitazone HCl salt in binary and multicomponent tablets	SRS in combination with chemometrics was used to quantify salt disproportionation in tablets

2.4.4 Multivariate data analysis

The differences in spectroscopic data from different solid-state forms are often subtle as they mostly originate from a different environment (neighboring molecules), rather than from the molecules themselves. In the case of polymorphs, the difference is in packing or conformation of molecules within the unit cell, whereas in the case of the amorphous form the neighboring molecular environment is disordered, giving rise to broader, less-defined peaks.[76] Additionally, molecules in the amorphous form can have a wider range of conformations themselves. These resulting subtle spectral differences are often difficult to detect visually, which is why multivariate data analysis is often required.[138] Moreover, as a powerful statistical tool, multivariate data analysis can handle large sets of data.

Principal component analysis (PCA) is one of the most commonly used multivariate methods in pharmaceutical research[1, 139, 140] and in the context of this thesis. PCA reduces the numerous independent or co-dependent measurement (in this case spectral wavenumber) variables to much fewer (often two or three) principal components (PCs), which describe the largest variance in the spectral data set. The spectral regions with highest variance can be traced back to the reference spectra via the loadings plot. The resulting scores plot depicts each spectrum as a point in a 2D or 3D space. Spectra that are more similar to one another are located closer together. PCA is a qualitative and unsupervised method, meaning that any sample groupings in the scores plot are based on the nature of the spectral data alone, with no prior input knowledge influencing the grouping.

2.5 Critical quality attributes (CQA)

A simplified definition of critical quality attribute (CQA)[141] implies any property of an output pharmaceutical material (API, excipient, intermediate material or finished drug product) that should be within certain limits in order to ensure desired product quality (quality target product profile). In pharmaceutical quality by design (QbD), input critical material attributes (CMA) and critical process parameters (CPP) are linked to an output CQA.[142] For solid dosage forms, CQAs typically include properties affecting product purity, strength, stability and drug release. This thesis focuses on physical storage stability and drug release of amorphous drug systems.

2.5.1 Storage stability

As the main hurdle in the wider application of the amorphous drug form is the propensity for crystallization (recall the unstable ball on top of an energy maximum), physical stability during storage is probably the most important and most commonly monitored CQA for amorphous samples. Performance during storage is routinely tested, for both the APIs and drug products. According to The International Conference on Harmonization (ICH) guidelines, the performance is tested at 25°C/60%RH (long term stability) for the duration of the product shelf life and at 40°C/75%RH (accelerated stability) during six months. If the accelerated stability study results are unsatisfactory, the intermediate conditions of 30°C/75%RH are introduced. In the case of amorphous drug formulations, in addition to chemical stability, the link between storage conditions and the physical state of the drug (referring to different degrees of order (amorphous versus crystalline) and molecular mobility) becomes highly important.

For a long time the rule of thumb for solid-state stability during storage of an amorphous drug was T_g−50 K.[143] Molecular mobility at temperatures 50 degrees below the T_g was believed to be negligible and insufficient to lead to crystallization.[20] More recently, it was found that it is not the T_g α, an indicator of global (whole molecule and cooperative) mobility, which helps in predicting the "safe" storage temperatures for the amorphous drugs. Rather, the T_g β, an indicator of local mobility (such as a side chain rotation) is the temperature that can more reliably predict the storage temperatures at which the crystallization is highly unlikely to occur.[21, 144-146]

In addition to elevated temperatures, the shelf life includes the effect of potential exposure to elevated humidity as well. Typically, the water vapor acts as plasticizer which lowers the T_g of the amorphous materials.[8, 28] While the storage temperature remains the same, a lower T_g of the drug in practice means a higher mobility and propensity for crystallization.

In the case of dosage forms, it is not only the influence of storage conditions on the drug that has to be taken into account. Rather, the interactions between drug and excipients, and the implications of elevated temperature and humidity on excipients, particularly on those amorphous in nature, such as polymers, have to be considered.[147, 148] This is particularly important since the mobility of polymer chains (assessed by measuring polymer's T_g) was

found to have a more important role in stabilization of the amorphous drug form than strength of interactions with the drug.[33]

2.5.2 Drug release

2.5.2.1 Dissolution behavior of amorphous drugs

Drug release is arguably the most important CQA of pharmaceutics. The ultimate goal of utilizing the amorphous drug form is to benefit from its improved apparent solubility, [13, 14] dissolution rate and bioavailability. However, as is the case with exposure to water vapor during storage, exposure to an aqueous environment during processing (e.g. granulation, coating), *in vitro* dissolution testing or *in vivo* (upon administration) can also facilitate the onset of crystallization.[138, 149-151] Solvent-mediated transformations occur when a metastable (more soluble) form converts to a more stable (less soluble) form as a result of supersaturated conditions at the dissolving surface or in the bulk solution.[152] Crystallization is thermodynamically favored; however, the kinetics determines whether the crystallization will occur in a time frame relevant for absorption.[151] Typically, the kinetics of solvent-mediated transformations are faster than direct solid state transformations. In this manner, the solubility advantage of the amorphous form is often lost.

Phase transformations occurring during the dissolution of the amorphous form can be described in three stages. Firstly, the amorphous form dissolves at a constant rate and the concentrations can become *supersaturated*, i.e. reaching values above the solubility of the crystalline counterpart. The term *solubility* implies amount (quantity) of solute dissolved at a given solvent. The maximum concentration achieved during supersaturation with respect to the *equilibrium solubility* of the stable crystalline form is often termed *apparent solubility*.[13] Next, a transformation stage with a decrease in concentrations begins. In this stage, enough of the organized clusters of the dissolved drug molecules reach their critical size (*nucleation*), and precipitation from the solution starts. As all surfaces can act as good nucleation sites, nucleation can easily occur at the (amorphous) drug formulation surface. Subsequent addition of the dissolved molecules to the growing crystal lattice (*crystal growth*) covers the amorphous surface with a more stable and less soluble crystalline coating. The crystal growth on the surface exposed to the dissolution medium inhibits the dissolution of the remaining underlying amorphous form. Finally, the steady-state phase starts when concentrations over time reach nearly constant values.

The *level of supersaturation* (the difference between the actual concentration and the solubility at a given temperature) is the driving force for crystallization. Thus ironically, maximizing the solubility advantage increases the potential for a solid-state transformation during dissolution.[153] Level of supersaturation also influences the nature of the crystalized form. Typically, higher levels of supersaturation result in faster precipitation and formation of metastable polymorphs whereas lower levels of supersaturation result in slower precipitation which allows time for the growth of more stable polymorphs.

Recrystallization during dissolution leads back to the problem of poorly water-soluble drugs[149] and is thus undesirable. Ideally, supersaturation should last long enough so that the

API can be absorbed. One strategy to prevent or delay recrystallization during dissolution is to use polymers. The presence of a polymer during dissolution is expected to provide a *parachute effect*, i.e. the maintenance of supersaturated concentrations formed by the rapidly dissolving amorphous form (the *spring*).[154] The parachute effect is primarily achieved by inhibition of drug precipitation (solution-mediated crystallization) and is more pronounced with SDs than with predissolved polymers.[155] Precipitation is inhibited by drug-polymer intermolecular interactions and/or steric hindrance. For instance, by adsorbing onto growing crystal faces, polymers can prevent the access and further deposition of drug molecules. Moreover, the increased viscosity due to the presence of polymer can also hinder diffusion of drug molecules from the bulk solution to the surface or already formed crystal nuclei.[156] Other mechanisms may support precipitation inhibition by polymers. For instance, the increase in the equilibrium solubility by the co-solvent effect can reduce the supersaturation and driving force for solution-mediated crystallization.

A good way to measure dissolution rate from amorphous formulations is to do intrinsic dissolution tests. In these measurements, a constant surface area allows evaluation of solid-state effects while minimizing the influence of particle size.[157] An intrinsic dissolution profile is typically depicted as a function of the cumulative amount of dissolved drug (concentration) versus time. Typically, if such a profile generates a straight line (under sink conditions), no phase transformations are taking place.[151] The dissolution rate is represented by the slope (derivative) of this line. In contrast, if a profile is curved, it is likely that a solution-mediated phase transformation has taken place.[151] This can be explained by the Noyes-Whitney equation (**Equation 4**), in which dC/dt is the dissolution rate, A is the surface area, D diffusion coefficient, h diffusion layer thickness and C concentration in (bulk) solution.

(4) $$\frac{dC}{dt} = \frac{DA(C_s - C)}{h}$$

If all other parameters stay the same, the decrease in C_s (solubility at the surface), caused by conversion of amorphous to crystalline solid, will decrease the dissolution rate in proportion with C_s. In contrast, if no transitions are occurring, C_s and consequently the rate remains the same. Sink conditions imply that $C_s >> C$. As the intrinsic dissolution testing implies a constant surface area (A), enlargement of the surface area due to solution-mediated crystallization must also be considered.

2.5.2.2 Solid-state analysis coupled with dissolution testing

The three-stage process of dissolution described above is a simplified representation. In reality, there could be many competing processes occurring simultaneously in the dissolution vessel or the gastrointestinal tract (GIT). To start with, the recrystallization itself may be to a crystalline form of the drug that is not necessarily the most thermodynamically stable form.[138, 149] In fact, according to Ostwald's rule of stages,[121] it is more likely that a metastable (the least stable) polymorph is obtained at first, which may be followed by a series of polymorph conversions.[1] Moreover, recrystallization may yield multiple

polymorphs, which may form simultaneously as polymorph mixtures.[14] The formation of hydrates[119, 158] and salts is also very common, and chelation is also possible.

Hence, it is not enough to monitor just drug concentrations in the solution, and try to draw conclusions from the trends in concentration that may indicate solid-state transformations. To better understand the process, dissolution testing can be coupled with a solid-state analysis technique[153] such as Raman spectroscopy[138, 149, 158] or microscopy,[150] ATR-FTIR spectroscopy,[77] ATR imaging,[78] or XR(P)D.[81, 149] The extent of solid-state transformations during dissolution is highest at the surface, which is in intimate contact with the aqueous environment.[81] The solid-state form of the drug surface also governs the solubility at the surface and therefore the dissolution rate. Thus, the selected solid-state analysis method should probe first and foremost the surface.

2.6 Why spectroscopic and nonlinear imaging?

Spectroscopic imaging offers contact- and label-free, non-destructive visualization of different solid-state forms. Spatially resolved imaging methods are preferred over bulk analysis, since solid-state transformations often imply changes in the crystal habit that could be visualized in a chemically- (and solid-state-) selective manner. Moreover, imaging methods can reveal any potential spatial distribution patterns of the different components within pharmaceutical formulations. Thus, spectroscopic imaging can help in answering several key questions, such as:

- Where is the drug (and other formulation components)?
- Which chemical and solid-state forms (of the many possible, and only some listed in **Figure 1**) are present?
- Are there any interactions between them?

This is because multiple spectra from different locations within the measured area are collected, as opposed to collection of a single spectrum that represents an averaged signal of the whole area measured. Nonlinear imaging can help answer the questions above in a *surface-specific* manner (and with up to video-rate imaging and sub-micron spatial resolution). Lastly, seeing is believing.

3 Aims of the study

The overall aim of this thesis is to utilize relatively novel, surface specific imaging techniques to better understand surface solid-state behavior. This platform is then used to establish the importance of surfaces in the crystallization, dissolution and stabilization of amorphous drugs.

More specifically, the objectives of this thesis were:

1. To establish a surface and solid-state specific imaging method capable of distinguishing multiple solid state forms at the surface (**I** and **II**)
2. To utilize the established imaging approach in comparing surface and bulk crystallization, as well as in monitoring stability of neat drugs and the effect of excipients on drugs' stability during storage (**I**, **II** and **IV**)
3. To investigate the effect of storage-induced changes on dissolution performance of neat and polymer-stabilized amorphous drugs (**III** and **IV**)

4 Experimental

4.1 Materials (I-IV)

Griseofulvin (polymorph I) was obtained from Sigma Aldrich (Sigma Aldrich, St. Louis, Missouri, USA) (**I**). Indomethacin (the γ form) was obtained from Orion, Espoo, Finland (**II**-**III**) or Hovione FarmaCiencia SA, Loures, Portugal (**IV**). The polymer excipients: hydroxypropyl methylcellulose acetate succinate MF (HPMCAS, Shin-Etsu Chemical Co., Tokyo, Japan), microcrystalline cellulose NF PH105 (MCC, FMC BioPolymer, Brussels, Belgium) and polyethylene glycol 6000 (PEG, Sigma-Aldrich, St. Louis, Missouri, USA), were used in binary mixtures with amorphous griseofulvin (**I**). PVP K30 (M_w 40 000) was obtained from Sigma Aldrich (Sigma Aldrich, St. Louis, Missouri, USA), and used as a polymer coating for amorphous indomethacin (**IV**).

4.1.1 Sample preparation and storage

In publications **I**-**III**, amorphous griseofulvin and indomethacin tablets were prepared by quench cooling melted drug powders with liquid nitrogen (griseofulvin) (**I**), or cooling to room temperature (indomethacin) (**II**-**III**), grinding the glass into a powder and compressing in molds. The tablets were then stored at 30°C/0%RH (griseofulvin) (**I**) or 30°C/23%RH and 30°C/75%RH (indomethacin) (**II**-**III**). A manual hydraulic press (Specac Ltd, Orpington, UK) was used for compression (**Figure 5**). In publication **IV**, the melt was cooled to 5°C, and amorphous indomethacin compacts were prepared by vacuum compression molding (MeltPrep® GmbH, Graz, Austria). This was followed by storage at 30°C/75%RH (**Figure 6**). The α,[159] ε[1, 160] and δ[161] polymorphs of indomethacin were prepared according to the methods in the corresponding above-mentioned references.

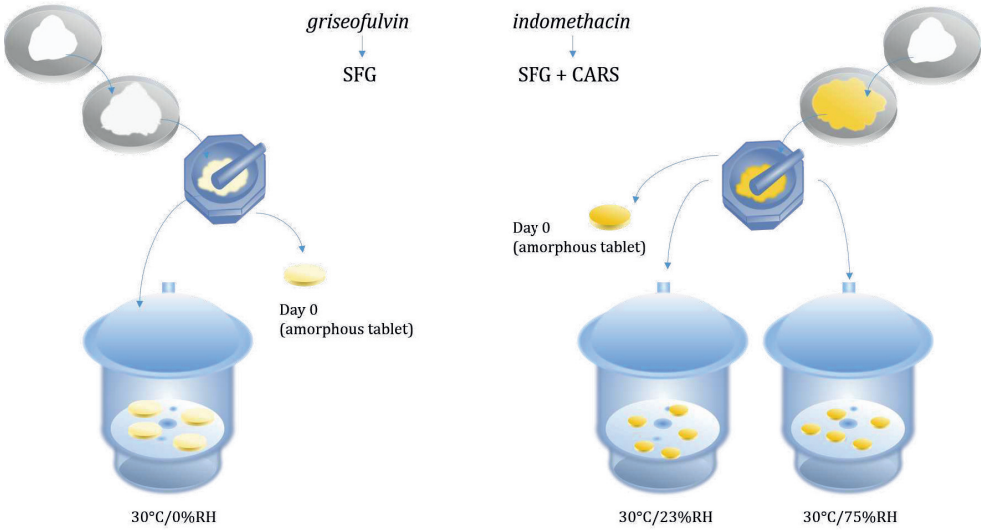

Figure 5 *Schematic representation of amorphous tablets preparation and consequent storage in publications **I** (griseofulvin), **II** and **III** (indomethacin): the amorphous form was prepared from crystalline powder by cooling the melt, then pulverized and compressed into tablets which were analyzed freshly and after storage at different conditions.*

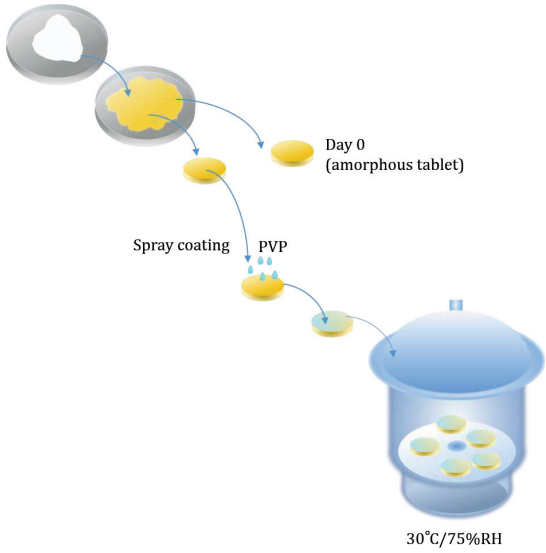

Figure 6 *Schematic representation of preparation, coating and consequent storage of amorphous indomethacin discs in publication **IV**: the amorphous form was prepared from crystalline powder by cooling the melt, then compressed into discs (with no grinding) which were analyzed; followed by spray-coating with PVP, storing, and analysis after storage.*

Tablets containing binary powder mixtures (1:1 w/w) of amorphous griseofulvin and polymers (HPMCAS, MCC and PEG) were prepared in the same manner as pure amorphous griseofulvin tablets (**I**), and stored at 30°C/0%RH. Multicomponent tablets containing an equal ratio of powdered amorphous, γ and α indomethacin (1:1:1 w/w) were prepared in the same manner as amorphous indomethacin tablets (**II**), with the exception that the relevant powders were physically mixed prior to compression.

4.1.1.1 Spray coating (IV)

In one study (**IV**), amorphous indomethacin compacts prepared by vacuum compression molding were spray coated with PVP (**Figure 6**). Spray coating with 0.5% w/v PVP solution was performed using a spray coater (Exacta Coat Ultrasonic Spraying system, Sonotec, Milton, New York, USA). One of the faces of each of the compacts was coated, with either two (2C) or ten (10C) spraying cycles, in order to obtain coatings with a thickness in the range of hundreds of nanometers and a micrometer, respectively. Coated samples were stored at 30°C/75%RH.

4.2 Methods

4.2.1 Solid-state characterization techniques

4.2.1.1 SEM (I-IV)

Powders and tablet sections (surfaces or cross-sections) were mounted on stubs using double-sided carbon tape. Samples were sputter coated with platinum. Microscopy was performed with a FEI Quanta™ 250 field emission gun SEM (FEI, Hillsboro, Oregon, USA) microscope using high vacuum and a voltage of 3-10 kV.

4.2.1.2 XRD (III-IV)

XRD measurements were performed using a Malvern Panalytical Empyrian (PANalytical B.V. Almelo, The Netherlands) instrument with Cu $K\alpha_1$ radiation (λ=1.5406). The generator voltage was 45 kV and the tube current 40 mA. Measurements were collected in a 2θ scan range of 5 to 50°. The compacts were spun during the measurements.

4.2.1.3 DSC (II-IV)

DSC measurements were performed on a DSC823e instrument by Mettler Toledo AG, Greifensee, Switzerland. Powder samples were gently pressed to cover the bottom of aluminum pans with pierced lids. The samples were heated from 25°C to 180°C at a rate of 10°C/min. Nitrogen was used as a purge gas with a flow rate of 50 ml/min.

4.2.1.4 ATR-FTIR spectroscopy (I-IV)

FTIR measurements were performed using a MIRacle ATR crystal (Pike Technologies, Fitchburg, Wisconsin, USA) mounted on a Vertex 70 spectrometer (Bruker Optics, Ettlingen, Germany). Each spectrum consisted of an average of 64 (**I**) or 256 (**II-IV**) scans with a spectral resolution of 4 cm^{-1}. Where applicable, the spectra were transformed using standard normal variance (SNV) prior to PCA.

4.2.1.5 Raman spectroscopy (II)

Raman spectra of indomethacin powders and tablet surfaces (**II**) were collected with a time-resolved Raman instrument (TimeGated® TG532 M1, Timegate Instruments Oy, Oulu, Finland) with fluorescence suppression. The excitation source was a 532 nm picosecond pulsed laser. The detector was a time-gated complementary metal-oxide semiconductor (CMOS) single-photon avalanche diode (SPAD) detector. Spectra of indomethacin powders were measured using a probe, while the tablet surfaces were measured by focusing the laser beam with a 40× microscope objective.

4.2.1.6 Nonlinear optical imaging (I-III)

Nonlinear optical imaging was performed using a commercially available fully integrated Leica SP8 CARS microscope (Leica Microsystems GmbH, Wetzlar, Germany). A dual-wavelength picoEmerald light source (A.P.E. GmbH, Berlin, Germany) was used for the CARS and SFG/SHG excitation. In this system, a Nd:YVO_4 laser output at 1064.5 nm was used as the Stokes excitation beam. The output from an optical parametric oscillator (OPO) was tunable in the range of 780–940 nm (limited by Leica optics) and was used as the pump/probe beam. The two laser beams were focused on the sample using an IR corrected 25x water immersion objective with NA of 0.95. The beams were spectrally and temporally overlapped in the tight focal volume. This configuration allowed for probing CARS frequencies in the range of 1240–3425 cm^{-1}. In general, the use of near infrared laser beams (longer wavelengths), such as in this set up, minimizes autofluorescence and photo-bleaching (sample damage) while simultaneously allowing deeper imaging due to lower scattering.[95] The emitted signals were collected in epi (backscattered) detection using photomultiplier tubes (PMT) and hybrid photodetectors (HyD). CARS spectral scans were obtained by tuning the pump line in 1 nm steps corresponding to frequency steps of around

12 cm^{-1}, while keeping the optical power constant. The emission spectra of the second order nonlinear signals (SFG/SHG) were collected by scanning the detection band with 10 nm steps. Reflected light bright field images were captured by using a 633 nm HeNe laser and a PMT detector.

SFG imaging of griseofulvin (**I**) was performed by detecting the signal at 450–470 nm. Nonlinear imaging of indomethacin (**II-III**) involved narrowband and hyperspectral CARS, SFG/SHG imaging and collection of second-order nonlinear spectra. Narrowband CARS images were obtained by overlapping channels with peak intensities of preselected single CARS lines, such as 1701 cm^{-1} in red (γ indomethacin), and 1676 cm^{-1} in blue (amorphous indomethacin). Where applicable, these channels were further overlapped with SFG/SHG signal in green (α indomethacin) (**II**), or channels with signals that satisfied a certain set of conditions (the CARS peak at 1652 cm^{-1} and SFG signal characteristic for α indomethacin were colored green, while a CARS peak at 1676 cm^{-1} and SFG signal characteristic for ε indomethacin were colored yellow) (**III**). Hyperspectral imaging included collection of CARS spectral scans in the 1413–1800 cm^{-1} range. Spectra were plotted as such (**II-III**) or further processed by PCA (**II**). Lastly, second order nonlinear spectra (400–700 nm) containing both the SHG signals and the SFG signal (resulting from the two different excitation wavelengths) were used to confirm the nature of nonlinear processes. In publication **II**, these spectra were used to extract pure SFG signal at 480–490 nm, which represented α indomethacin and was then presented in yellow color. The colors used in the final images are arbitrary due to the software used in the data collection and analysis.

4.2.2 Intrinsic dissolution testing (III-IV)

Intrinsic dissolution tests of fresh and stored indomethacin samples were performed in phosphate buffer at pH 6.8 at room temperature (**III**) and at 37°C (**IV**). Tests were performed at least in triplicate. The absorbance of unfiltered samples at specific time points was measured at 318 nm with UV spectrophotometry (UV-1600PC UV–Vis spectrophotometer, VWR International, Shanghai, China). A custom built channel flow set up used in publication **III** was similar to that of Peltonen et al.[162] The tablets were fixed in the cavity of the channel flow cell, so that only one surface was exposed to buffer. A constant flow of fresh buffer (9 ml/ml) was supplied by a peristaltic pump (505U, Watson Marlow, Falmouth, England), which ensured true sink conditions. Intrinsic dissolution tests in publication **IV** were performed in a paddle apparatus in 900 ml of medium at 50 rpm (Erweka DT6, Erweka GmbH, Langen, Germany). Intrinsic conditions were ensured by coating one flat surface and the radial surface of compacts with nail polish (Mavala Switzerland base coat) containing waterproof agents. In both studies, at the end of dissolution testing (15 minutes, **III**, or 45 minutes, **IV**) the compacts remained whole, which enabled further solid-state analysis.

5 Results and discussion

5.1 Surface specific imaging of multiple solid-state forms and their transformations (I and II)

In this section, non-linear imaging methods for sensitive detection of surface crystallization were established. Firstly, SFG was utilized to detect compression-induced surface crystallization of amorphous drug to a single polymorph. Secondly, two imaging modalities based on multimodal non-linear imaging (combination of SFG and CARS) were developed in order to discriminate the amorphous and two crystalline polymorphs of the same drug at the surface of three-component tablets.

5.1.1 Detecting a single phase transition with SFG

For pharmaceutical formulation development, it is important to be able to detect solid-state changes during and after different manufacturing steps, such as compression. In contrast to bulk spectroscopic methods, modern techniques allow for imaging of these changes, and this approach was used in this thesis. Amorphous griseofulvin typically crystallizes to polymorph I,[99, 115] which has a non-centrosymmetric structure belonging to the $P4_1$ space group.[163, 164] Thus, polymorph I generates a SFG signal, as opposed to the starting amorphous material. The presence or absence of SFG signal can therefore be used to monitor crystallization of the amorphous form to a single SFG active polymorph. This feature enabled insights into spatial distribution patterns of compression-induced crystallization in amorphous griseofulvin tablets. The distribution of compression-induced crystallinity was almost exclusively at the surface, with minimal crystallinity detected in the core. Well-established surface complementary characterization methods, SEM and ATR-FTIR analysis were compared to the SFG imaging. In comparison to these techniques, SFG was more sensitive in detecting compression-induced crystallinity at the surface. Immediately upon compression, only some of the tablets were found (partially) crystalline according to the ATR-FTIR analysis. SEM images showed smooth surface with an absence of branch-like features attributed to crystallinity. However, SEM does not directly probe the solid-state form and is thus prone to errors based on morphological interpretation. In contrast, crystallization was detected with SFG even in tablets that were classified as amorphous by ATR-FTIR spectroscopy and SEM (based on lack of crystal-like features). Further, SFG revealed that the distribution of crystallinity at the surface was not uniform, which was the likely cause for difference in results obtained by ATR-FTIR analysis.

SFG (including SHG) can be used independently to differentiate between different components based on the presence or absence of the signal or, in certain cases, the difference in signal intensity,[130] of several SFG active components. The fact that the amorphous materials or liquids do not generate a SFG signal can be conveniently exploited in monitoring crystallization from the amorphous form[101, 132] or from solution.[126, 133] However, in the qualitative analysis with SFG (including SHG), the utility of signal intensity alone

when characterizing multicomponent systems is limited. Furthermore, preferred orientation effects and the polarization-dependent SFG response may complicate analysis based only on signal intensity differences. Thus, in many studies SHG has been used as a rapid initial assessment method followed by independent analysis by Raman spectroscopy[100] and/or (synchrotron) XRD,[129] which provide additional chemical and improved solid-state specificity, as well as a theoretically linear dependency of signal intensity on concentration. Alternatively, SFG can be combined with another nonlinear optical method in correlative or multimodal[116, 123] imaging, as presented in the next chapter.

5.1.2 Differentiating multiple solid-state forms with multimodal nonlinear imaging

This part of the thesis focused on developing a method able to differentiate between three solid-state forms of indomethacin (the amorphous form and two crystalline polymorphs) at the surface of multicomponent tablets. One of the polymorphs, the γ form, has a centrosymmetric structure belonging to the $P\bar{1}$ space group,[165] while the other, the α form, belongs to the non-centrosymmetric $P2_1$ space group.[166] As described above, only non-centrosymmetric crystalline structures can generate a bulk SFG signal, with bulk SFG being impossible for centrosymmetric and disordered amorphous materials. In a system with three solid-state forms, out of which two are SFG inactive (γ and the amorphous form), SFG analysis alone would not have been sufficient to differentiate between all the forms. A multimodal imaging approach, in which SFG and CARS signals are simultaneously generated and sensitive to different solid-state forms in the sample, provided greater analytical power. This approach distinguished the α form based on its SFG activity and in addition allowed differentiation between the SFG inactive γ polymorph and the amorphous form, based on their characteristic CARS peaks. Different solid-state forms of indomethacin can be spectroscopically differentiated in the carbonyl-stretching region (1500-1800 cm^{-1}).[1, 60, 78] In this work, the γ polymorph was imaged using the CARS peak at 1701 cm^{-1} while the amorphous form was imaged at 1676 cm^{-1}.

Two multimodal imaging approaches were developed (**Figure 7**). Firstly, narrowband CARS and SFG/SHG imaging (**Figure 7a**) were correlatively combined. SFG/SHG consisted of the combination of the SFG (generated from the two different laser excitation wavelengths) and the two SHG signals at 465 ± 85nm, and was used to detect the α form (shown in green). Two single-frequency CARS lines, characteristic for the γ and amorphous forms, were represented in red and blue, respectively. Secondly, hyperspectral CARS and SFG imaging derived from second-order nonlinear spectra (from which SFG signal at 480-490 nm was extracted) and whole CARS spectra (1413 to 1800 cm^{-1}) was performed. Hyperspectral CARS imaging (**Figure 7b**) generates so-called spectral cubes in which each pixel (defined by *x* and *y* values) is associated with a CARS spectrum in the *z* direction. Spectra from all the pixels in the image were processed by PCA, and the first three PCs describing the highest variance were used to compress the image in the *z* dimension. Each of the PCs was assigned with a color: PC1 with red, PC2 with green and PC3 with blue. This approach reduced the data dimensionality from all probed CARS frequencies to only three PCs, as represented by the shrinking of the image cube in the *z* direction in the RGB

(red, green, blue) image (**Figure 7b**). Additionally, RGB layers were overlaid with the SFG signal (480-490 nm, in yellow), as opposed to the narrowband approach in which both the SFG and SHG signals (465 ± 85nm, in green) were used together.

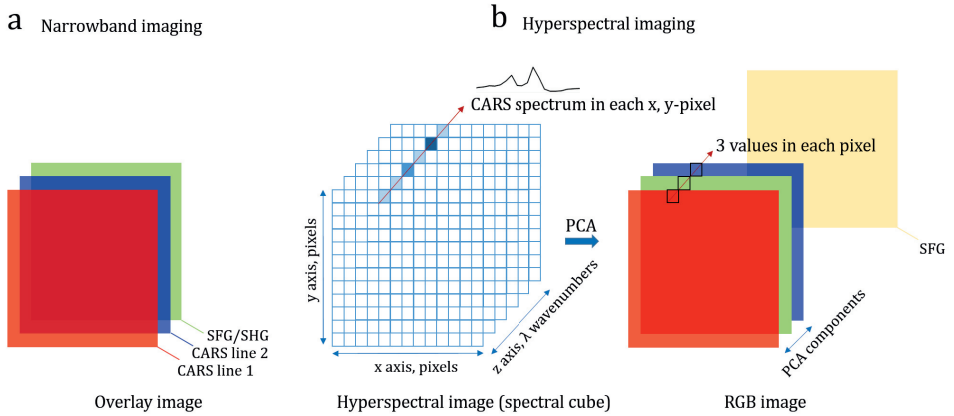

Figure 7 *Schematic representation of two nonlinear imaging modalities a) narrowband CARS and SFG/SHG imaging and b) hyperspectral CARS and SFG imaging, including conversion of hyperspectral CARS image to a PCA-based RGB image.*

Figure 8 provides a comparison of these two imaging approaches in tablets consisting of equal ratios of γ, α and amorphous indomethacin. The images provide similar color-coded information about distribution and identity of indomethacin solid-state forms. However, there are some important practical differences. The narrowband approach is much faster, and the images can be captured within seconds. All signals (selected CARS lines for amorphous and γ forms of indomethacin as well as the SFG/SHG signal of the α form) are pre-colored and do not require further processing. This approach however requires prior knowledge on the expected species and their characteristic CARS peaks or SFG activities. On the other hand, the hyperspectral approach involved considerably longer measurement times (depending on number of CARS frequencies probed) as well as PCA data processing time (the latter could be significantly shortened by automated software). Solid-state form assignments must be made based on inspection of the PC loadings. However, the hyperspectral approach can identify unexpected components, it does not require much prior knowledge about the sample properties (lower or higher CARS wavenumber region should be preselected) and can be utilized in complex mixtures such as pharmaceutical formulations, which may involve overlapping spectral features. Moreover, in this particular case, the hyperspectral approach included measurements of second-order nonlinear spectra (containing resolved SFG and both of SHG peaks) which could also unequivocally exclude any signal contributions from potentially present TPEF. Hyperspectral CARS imaging followed by PCA developed in this work was more recently applied by Ojarinta et al. to study crystallization in multicomponent tablets.[134]

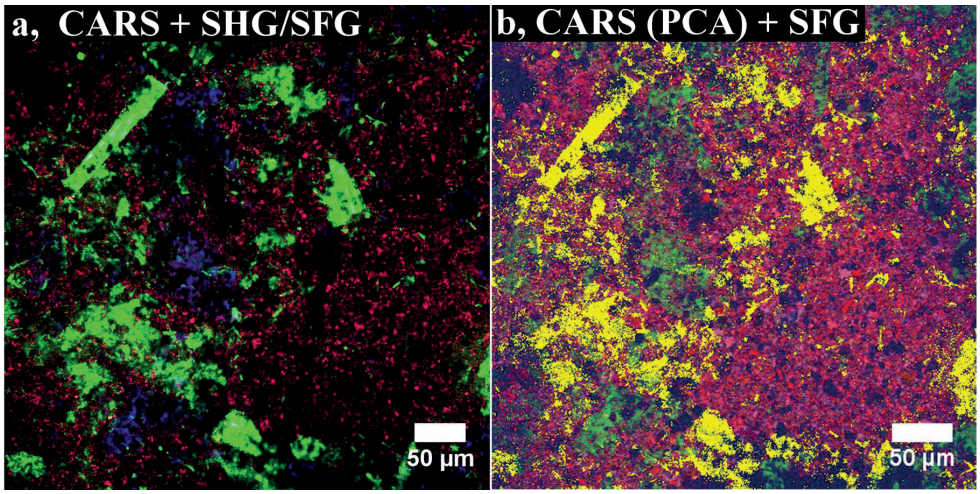

Figure 8 *Comparison of two nonlinear imaging modalities a) narrowband CARS and SFG/SHG imaging and b) hyperspectral CARS and SFG imaging in tablets consisting of equal ratios of γ, α and amorphous indomethacin. Color coding: a) γ indomethacin in red (CARS signal at 1701 cm^{-1}), amorphous indomethacin in blue (CARS signal at 1676 cm^{-1}) and α indomethacin in green (SFG/SHG signals at 465 ± 85 nm); b) RGB assignments based on PC loadings are available in Appendix II: γ indomethacin in red (PC1), amorphous indomethacin in green (PC2); α indomethacin in yellow (SFG signal at 480-490 nm). Reprinted with permission from publication **II**. Copyright 2017 American Chemical Society.*

5.2 Stability during storage (I, II and IV)

After the analytical method for studying solid-state changes with SFG and CARS was established, its usability in monitoring crystallization during storage (as one of the main CQAs) was demonstrated. In this part of the thesis, the stability of amorphous drug in different storage conditions was monitored. The performance of neat drug versus *a)* binary mixtures of drug with the polymers and *b)* amorphous drug coated with thin polymer layers was compared. Crystallization was monitored by SEM, ATR-FTIR spectroscopy, XRD, Raman microscopy and nonlinear optical imaging. SFG analysis was used to monitor the progression of compression-induced surface and bulk crystallization during storage and determine the influence of polymer excipients thereof. Multimodal non-linear imaging (combining SFG and CARS) was applied to monitor storage-induced surface crystallization of amorphous drug to two polymorphic forms.

Two distinct amorphous systems were studied: a) tablets made from compressed powder (**I**, **II**, (and **III**)) and tablet-like discs (**IV**). The main difference between these systems is the structure within the bulk/core. A tablet made from compressed grinded powder includes many interfaces and surfaces within the bulk, which can influence the crystallization. In contrast, tablet-like discs can be thought of as a single, continuous amorphous particle.

5.2.1 Neat drug

5.2.1.1 Surface versus bulk crystallization of griseofulvin

The SFG method implemented for detecting compression-induced crystallization was further utilized to monitor the crystallization of amorphous griseofulvin (compressed powder) tablets during storage at 30°C/0%RH (**Figure 9**). Moreover, the hypothesis tested here was whether the crystallization would be surface-biased. Bright field images show reflection of the laser light and depict (in grey color) the whole area of the tablet that was imaged. In the SFG images, green color indicates crystalline areas where the SFG signal is generated. SFG signal at the surface and in the cross-sections (cut tablets) was compared in a qualitative manner. The crystalline drug was primarily distributed at the surface. Crystallization continued to be surface-biased throughout the storage time studied and in the case of bulk visualized in the tablet-cross-sections, crystalline regions were closer to the edges of compacts (**Figure 9**). The images suggest that the increase in crystallinity at the surface during storage was faster than that in the bulk. Therefore, the tested hypothesis was correct.

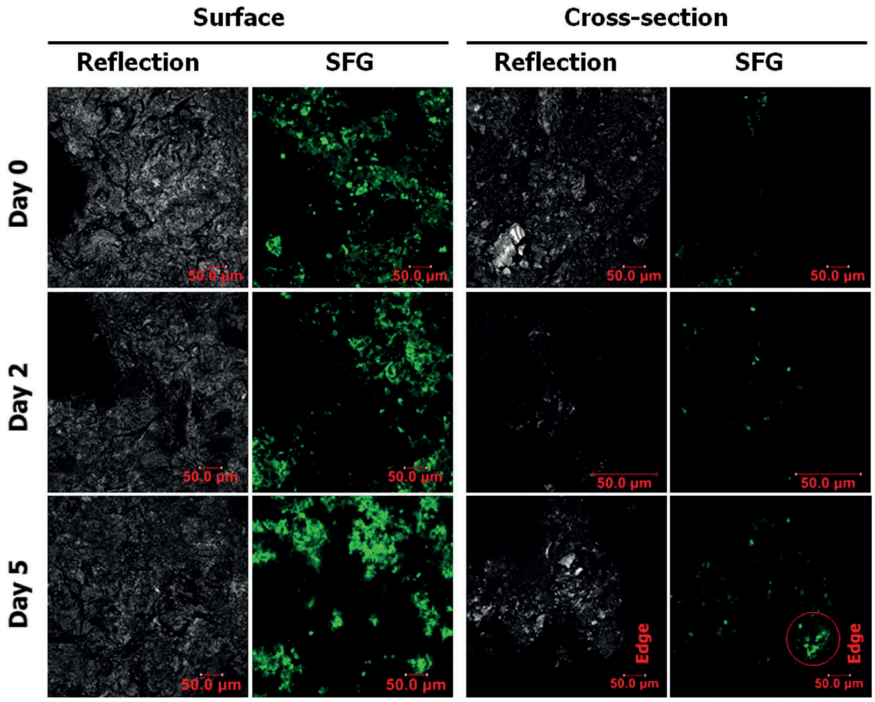

Figure 9 *Reflection and SFG images of surfaces and cross-sections of amorphous griseofulvin tablets during storage at 30℃/0%RH. Imaged tablets were found amorphous according to ATR-FTIR and SEM analyses on Day 0. Green color indicates SFG active crystalline regions. Reprinted by permission from Springer Nature, publication **I**, copyright 2016.*

5.2.1.2 Surface crystallization of indomethacin

The physical stability of amorphous indomethacin (compressed powder) tablets during storage at 30°C/23%RH and 30°C/75%RH was assessed with SEM, ATR-FTIR spectroscopy, Raman microscopy and multimodal nonlinear optical imaging. As expected from previous studies,[31] the amorphous indomethacin crystallized to different solid state forms depending on the humidity. At the lower humidity, the crystallization yielded primarily the γ form of indomethacin whereas at the elevated humidity, the α polymorph was dominant. Initial crystallization started quite soon in the stability tests and was fully apparent after 1-3 weeks, depending on the analysis technique used. This further highlights the inherent instability of the amorphous form during storage.

In comparison with the ATR-FTIR spectroscopy and Raman microscopy analyses, multimodal nonlinear imaging (**Figure 10**) provided additional information. In many images, multiple forms (two polymorphs and the amorphous form) were resolved simultaneously, in contrast to the ATR-FTIR and Raman analyses where the signal was averaged over a larger sampling volume and fewer forms could be differentiated (even with the aid of PCA). Further, multimodal nonlinear imaging was more sensitive when compared to ATR-FTIR spectroscopy and Raman microscopy analyses and detection of crystallization to both polymorphs was observed at an earlier stage, already by days 1 and 2. In contrast, the earliest time point where crystallization could be detected with ATR-FTIR spectroscopy and Raman microscopy was day 5 at 23%RH, and even then only the dominant γ polymorph was detected. However, at 75%RH, the α form was detected with ATR-FTIR analysis only at day 22, while the Raman microscopy could not clearly reveal this form (most likely due to lower axial resolution and a more limited sampling area). Lastly, minority species were detected amongst the prevalent polymorph with nonlinear imaging. For instance, traces of the α form were identified in almost exclusively γ crystalline areas after storage at low humidity (as shown in spot 9 in **Figure 10a**). CARS spectral scans (**Figure 10d**) additionally confirmed the presence of minority species. Simultaneous use of SFG and CARS techniques improved solid-state specificity compared to one nonlinear analysis technique alone. For instance, SFG is very sensitive to non-centrosymmetric crystals, such as the α form of indomethacin, which is the weakest Raman scatterer of the three studied solid-state forms. Moreover, CARS distinguished solid-state forms that could not have been resolved using SFG only. Hence, the two techniques synergistically complemented one another. Even though transient solid-state changes were not detected directly, they could be assumed by, for example, the disappearance of small α crystalline areas at the expense of the growing γ polymorph crystals at 23%RH, in accordance with the system gravitating towards the energy minimum.

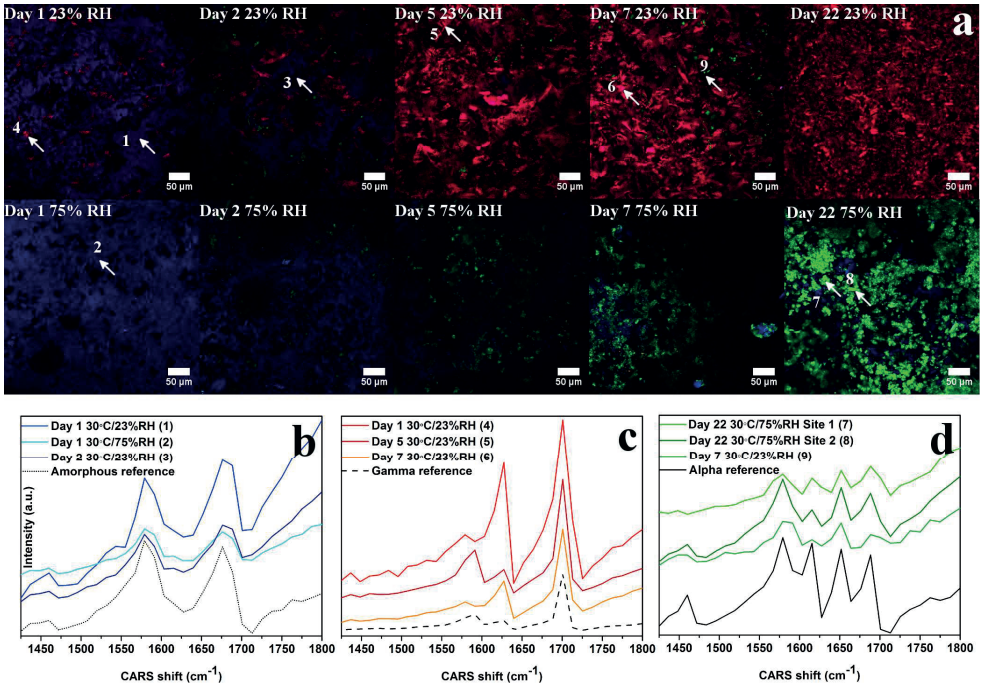

Figure 10 *Nonlinear narrowband CARS and SFG/SHG imaging of amorphous indomethacin tablets during storage at 30°C/23%RH and 30°C/75%RH a). Color-coding: a) γ indomethacin in red based on the CARS signal at 1701 cm^{-1}, amorphous indomethacin in blue based on the CARS signal at 1676 cm^{-1} and α indomethacin in green based on the SFG/SHG signals at 465 ± 85 nm. CARS spectra from specific regions of interest (marked with an arrow and a number) are depicted in panels b), c) and d), together with spectra of reference indomethacin solid-state forms imaged as powders. Reprinted with permission from publication* ***II****. Copyright 2017 American Chemical Society.*

5.2.2 Influence of polymer excipients

To investigate the influence of polymer excipients on the surface and bulk crystallization of amorphous griseofulvin, (compressed powder) compacts consisting of binary physical mixtures of griseofulvin with HPMCAS, MCC and PEG were prepared. It was expected, that the excipients would either promote or hinder crystallization. The studied polymers did not exhibit detectable SFG signal, with only the crystalline form of griseofulvin (polymorph I) conveniently generating a significant SFG signal. Different excipients combined with amorphous griseofulvin did not reduce the initial levels of compression-induced surface crystallization detected immediately upon preparation. In fact, PEG was found to promote both the surface and bulk crystallization upon compression.

Upon storage at 30°C/0%RH for 2 days, HPMCAS and MCC differently affected the crystallization in the bulk. MCC appeared to promote bulk crystallization while HPMCAS suppressed bulk crystallization. PEG continued to catalyze crystallization. These observations are in accordance with previous studies where PEG was shown to be capable

of promoting crystallization in SDs[167] or as an excipient co-spray dried with lactose,[168] and HPMCAS being a well-known inhibitor in SD.[169] At the same time, none of the physically mixed polymers were able to mitigate the crystallization at the surface of the compressed tablets. Surface crystallization of amorphous drugs in contact with excipients (lightly compressed on top of amorphous glass films) was studied by Zhang et al.[170] Among other drug-excipient combinations, the authors studied indomethacin and nifedipine in contact with MCC, and found that MCC increased the crystallization levels of nifedipine, however no significant difference on crystallization of indomethacin was observed. The authors suggested that this effect was drug-specific.

5.2.3 Influence of polymer coatings

As discussed in the review of literature, thin polymer coatings are a promising tool for the stabilization of the amorphous drug form at the surface of drug particles, films or tablets, where the crystallization typically starts. This part of the work investigated the potential of PVP spray-coating in stabilizing amorphous indomethacin tablet-like discs during storage. This system is a coherent single-phase tablet (equivalent to a glass film) and does not comprise compressed grinded powder. As opposed to the study with griseofulvin, where we wanted to see the influence of different commonly-used compressed tablet excipients on enhancing or suppressing the crystallization, here the aim was to inhibit the crystallization. Thus PVP was selected as it is a well-known stabilizer of amorphous indomethacin when prepared as a solid dispersion.[36] The carbonyl group of PVP hydrogen bonds with the hydroxyl group of indomethacin which increases the physical stability.[60] Samples were stored at elevated temperature and humidity (30°C/75%RH).

To study the surface stabilization of amorphous drugs with thin polymer coatings, compacts resembling quench cooled amorphous glass rather than powder compacts were selected. Mechanical pressure during grinding and compression of powdered material, as well as any potential air pockets present in such compacts may enhance the crystallization throughout the material, with potential crystallization of the individual (partially-fused) particles forming the tablet. In contrast, the compacts obtained by vacuum compression molding (MeltPrep®) were single-phase continuous systems that were free of air bubbles and other interfaces. Furthermore, the tablet surfaces were smooth and the production process eliminated the need for grinding. This method of preparation is likely to resemble glasses obtained by traditional quench cooling of the melt, prior to grinding and compaction, and was also needed in order to obtain a uniform thin film coating. A recent study that compared quench cooled amorphous celecoxib discs prior to and after compression showed that both mechanical pressure and compression times affected destabilization of amorphous glasses.[30]

As an additional advantage, these discs enabled the visual confirmation of crystallization occurring during storage in the form of opacity (from translucent to opaque) and color changes (from yellow to white). The compacts had a relatively large surface area of 3.14 cm^2. Hence, the combination of ATR-FTIR and XRD methods was especially suitable for analysis. XRD reflection measurements while the compacts were spun provided information about the averaged solid-state form with surface-biased sampling (**Figure 11**), while the

ATR-FTIR measurements were done on a minimum of three targeted regions at the sample surfaces and provided even more surface-biased solid-state information. Furthermore, the amorphous PVP coatings were invisible to XRD, in contrast to ATR-FTIR analysis, which allowed for detection of PVP-water interactions, for instance.

Cross-section SEM images showed that the obtained PVP coatings had coating thicknesses of ~200 nm and ~1 µm for 2C and 10C, respectively. Moreover, SEM cross section images confirmed the surface-biased crystallization, this time in the tablet-like single particle amorphous samples (Appendix IV). As can be seen from the diffractograms (**Figure 11**), thin polymer coatings can delay the onset of crystallization under elevated temperature and humidity conditions. This effect depended on the coating thickness. Uncoated samples (N) had detectable levels of crystallinity already at day 3 (**Figure 11a**). Thinner coatings (2C) doubled this time, and first peaks superimposed on amorphous halo were visible on day 7 (**Figure 11b**). Thicker coatings (10C) provided protection up to day 14, double the time compared to that of the thinner coatings (**Figure 11c**). The main findings were confirmed with the ATR-FTIR spectroscopy (except that the PVP signal in thicker coatings dominated the spectra, which on the other hand allowed for detection of PVP-water interactions).

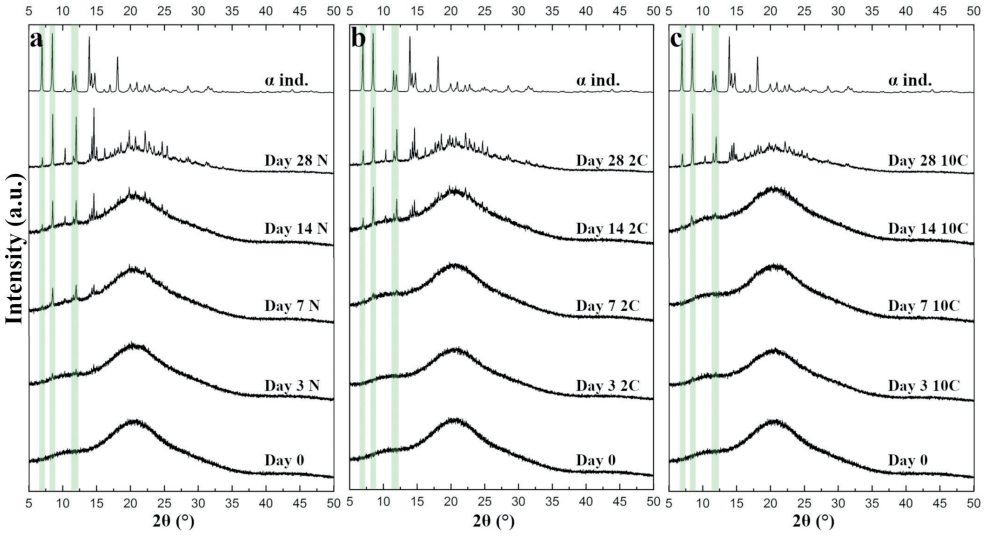

Figure 11 *X-ray diffractograms of a) uncoated and two types of PVP-coated amorphous indomethacin compacts: b) PVP-coated with two cycles (2C) and c) PVP-coated with ten cycles (10C).*

5.3 Stability during dissolution (III and IV)

In this part of the thesis, drug release as one of the main CQAs for solid dosage form was tested. Dissolution performance of neat amorphous indomethacin drug compacts

(compressed powders) as well as of amorphous indomethacin discs stabilized with thin polymer coatings (single amorphous particle) was assessed. The dissolution behavior was monitored and correlated to the stability studies and the different levels and nature of surface crystallinity present prior to dissolution. The effect of polymer coating thickness was also of interest. Solution-mediated crystallization was monitored by SEM, ATR-FTIR spectroscopy, XRD, Raman microscopy and multimodal nonlinear optical imaging. All tests were performed in phosphate buffer at pH 6.8.

5.3.1 Dissolution induced solid-state transformations resolved with multimodal nonlinear imaging

Once the surface-specific and solid-state sensitive method for the detection of surface crystallization was established and applied to study physical stability during storage, the next research question emerged. Naturally, it became important to know how this early stage surface crystallization affects the dissolution performance.

As can be seen from **Figure 12**, trace levels of storage-induced crystallization detectable with nonlinear imaging but not with ATR-FTIR spectroscopy and Raman microscopy (days 1 and 2) do not necessarily impair dissolution and supersaturation. It is important to note that the retardation of dissolution due to early stages of crystallization may be more significant in the case of other samples. In this study, the decrease in dissolution performance was significant only in the latter stages of storage (days 7 and 22) when the surface crystallization prior to dissolution was much more pronounced. The most significant difference in dissolution performance between different storage conditions (23%RH vs. 75%RH at 30 °C) was observed at day 7, when dissolution impairment was more pronounced following storage at 23%RH. This was in line with the earlier observed and faster trend of crystallization at this storage condition.

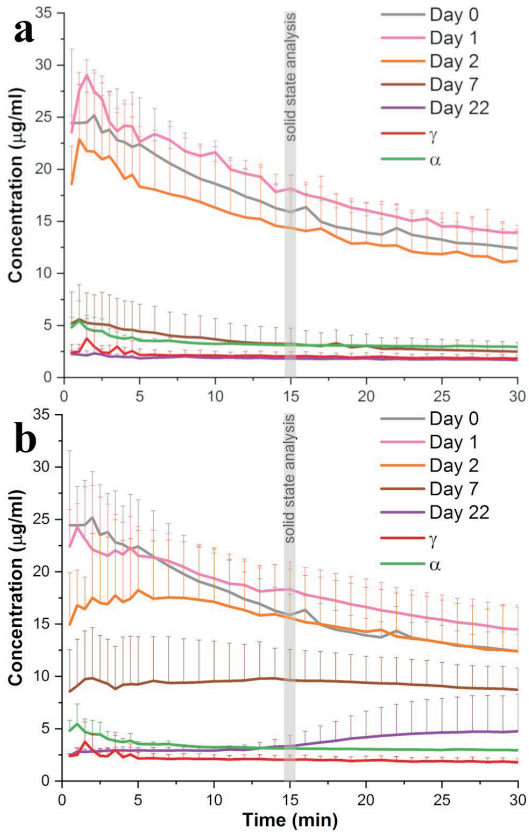

Figure 12 *Intrinsic dissolution profiles in phosphate buffer at pH 6.8 (mean of minimum three measurements) of amorphous indomethacin compacts stored at a) 30°C/23%RH and b) 30°C/75%RH. Profiles of reference crystalline α and γ forms are shown for comparison. Error bars represent plus one standard deviation. Reprinted with permission from publication **III** (https://pubs.acs.org/doi/10.1021/acs.molpharmaceut.8b00840). Further permissions related to the material excerpted should be directed to the ACS.*

Dissolution testing was accompanied by off-line solid-state analysis at the 15-minute dissolution time point and included SEM, XRD, ATR-FTIR spectroscopy and multimodal nonlinear optical imaging. All employed techniques indicated crystallization due to dissolution. Similar to the storage studies, multimodal nonlinear imaging was more sensitive and informative than other techniques employed, namely XRD and ATR-FTIR spectroscopy.

Nonlinear imaging revealed multiple simultaneously present solid-state forms on the surface of powder compacts that underwent dissolution (**Figures 13 and 14**). Many of the identified polymorphs were present only in trace amounts. In contrast, XRD and ATR-FTIR analyses provided averaged solid-state information with contributions from different components, which were fewer in number and required PCA processing in the case of ATR-FTIR spectroscopy (**Table 4**). In particular, nonlinear imaging simultaneously revealed up to five solid-state forms, four polymorphs (α, γ, ε and η) and the amorphous form upon

storage at elevated humidity for 7 days (**Figure 14b**). In contrast, the highest number of solid-state forms deduced from XRD and ATR-FTIR analyses was three (**Table 4**). As three (α, ε and η) out of these four simultaneously present polymorphs were SFG active, their differentiation was enabled by the synergistic use of both CARS and SFG. Of particular importance, hyperspectral CARS imaging allowed detection of minority polymorphs including the η form, which was not anticipated based on previous dissolution studies (with the same model drug and pH).[1, 150]

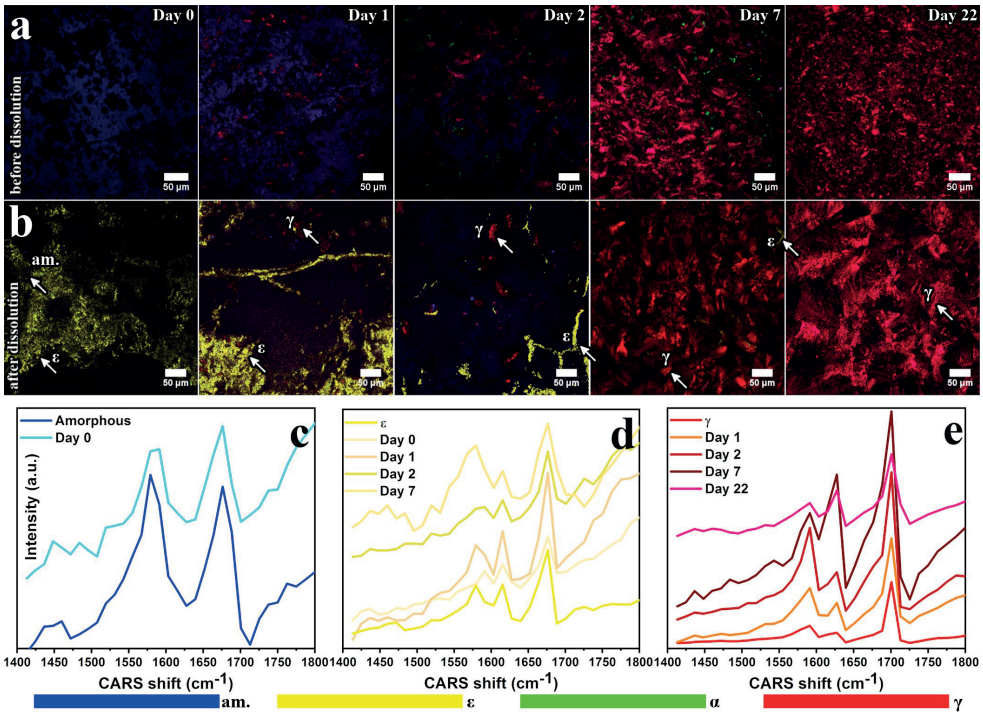

Figure 13 *Nonlinear optical imaging of amorphous indomethacin compacts stored at 30°C/23%RH a) prior to and b) upon intrinsic dissolution testing at pH 6.8 for 15 minutes. CARS spectra from certain regions of interest (marked with an arrow) are depicted in panels c), d) and e) together with spectra of reference indomethacin solid-state forms imaged as powders. Color-coding: γ indomethacin in red based on CARS signal at 1701 cm^{-1}, amorphous indomethacin in blue based on CARS signal at 1676 cm^{-1}, ε indomethacin in yellow based on SFG activity and CARS signal at 1676 cm^{-1} and α indomethacin in green based on SFG activity and CARS signal at 1652 cm^{-1}. Reprinted with permission from publication **III** (https://pubs.acs.org/doi/10.1021/acs.molpharmaceut.8b00840). Further permissions related to the material excerpted should be directed to the ACS.*

The number of detected solid-state forms depended on storage conditions. Generally, storage at higher humidity (75%RH) resulted in a higher number of detected metastable forms upon dissolution (**Table 4**). The ε and η forms were present only upon exposure to the dissolution medium, which indicated their crystallization was solely solution-mediated. Nonlinear imaging also revealed particular distribution patterns, such as more extensive

crystallization along cracks and pores on the surfaces of samples stored at 23%RH that underwent dissolution (**Figure 13b**). Recent work by Powell et al.[56] suggests that fractures and deformities might indeed play a very important role in crystal growth in general. The authors hypothesized that crystallization in the bulk also progresses through surface crystallization in constantly created voids and free surfaces.

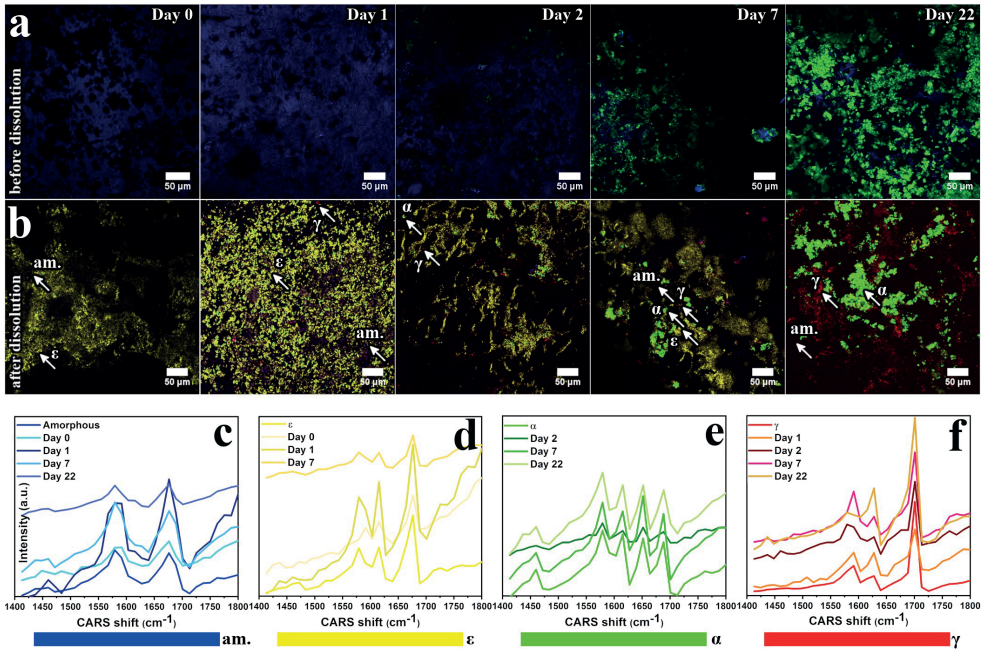

Figure 14 *Nonlinear optical imaging of amorphous indomethacin compacts stored at 30°C/75%RH a) prior to and b) upon intrinsic dissolution testing at pH 6.8 for 15 minutes. CARS spectra from certain regions of interest (marked with an arrow) are depicted in panels c), d), e) and f) together with spectra of reference indomethacin solid-state forms imaged as powders. Color-coding: γ indomethacin in red based on CARS signal at 1701 cm^{-1}, amorphous indomethacin in blue based on CARS signal at 1676 cm^{-1}, ε indomethacin in yellow based on SFG activity and CARS signal at 1676 cm^{-1} and α indomethacin in green based on SFG activity and CARS signal at 1652 cm^{-1}. The spectrum of η form is available in Appendix III. Reprinted with permission from publication **III** (https://pubs.acs.org/doi/10.1021/acs.molpharmaceut.8b00840). Further permissions related to the material excerpted should be directed to the ACS.*

Table 4 *Overview of the observed solid-state forms of indomethacin before and after 15 minutes of intrinsic dissolution testing. Reprinted with permission from publication **III** (https://pubs.acs.org/doi/10.1021/acs.molpharmaceut.8b00840). Further permissions related to the material excerpted should be directed to the ACS.*

Sample	Solid state					
	XRD		ATR-FTIR*		CARS/SFG	
	before	after	before	after	before	after
Day 0	am**	am, ε	am	am, ε (traces)	am	am, ε
30°C/23%RH						
Day 1	am	am, ε	am	am, ε (traces)	am, γ	am, ε, γ
Day 2	am, γ	am, γ	am, γ	γ	am, γ, α (traces)	am, ε, γ
Day 7	γ	γ	γ	γ	γ, α	ε, γ
Day 22	γ	γ	γ	γ	γ, α (traces)	γ
30°C/75%RH						
Day 1	am	am	am	am	am, α (traces)	am, ε, γ, α (traces)
Day 2	am, γ	am, γ, ε	am, γ	ε	am, α, γ (traces)	am, ε, γ, α
Day 7	am, γ, α	am, γ, α	am, γ	am, ε, γ	am, α, γ (traces)	am, ε, γ, α, η (traces)
Day 22	am, γ, α	am, γ, α	am, α	am, γ	am, α, γ (traces)	am, γ, α

*Tentative assignments based on IR spectra and PCA

**am=amorphous

Less well-studied polymorphs of indomethacin (ε, η and δ), whose crystal structures have not yet been published, as well as the α form, were further characterized as non-centrosymmetric crystals, based on their SFG activity (**Figure 15**). This information may be helpful in potential future structure determinations.

Even though this was not the main aim of this study, it was intriguing to detect this many polymorphs and further to be able to separate their spectra from a complex sample. **Figure 15** includes a comparison of Raman and CARS spectral features for all studied solid-state forms of indomethacin. As the signal arises from the same molecular vibrations, the spectra are uniquely related to one another. This figure also illustrates the lower spectral resolution of CARS spectra with the setup and collection parameters employed (the setup is optimized for rapid narrowband imaging rather than CARS spectra acquisition). In this study, the ε form after dissolution testing was observed mostly in samples that remained predominantly amorphous upon storage. Earlier studies[150, 171] also reported a Raman peak at 1670 cm^{-1} upon dissolution of amorphous indomethacin; however, this was not attributed to the ε form at the time and its solid-state origin was unassigned. Surwase et al.[1] reported and further characterized (with ATR-FTIR spectroscopy) this polymorph while studying amorphous suspensions in phosphate buffer at pH 6.8 and 1.2. In contrast, the authors observed the η form only at pH 1.2, possibly due to poorer detection limit of the ATR-FTIR analysis

compared with the nonlinear imaging. An ATR-FTIR spectrum of the ε form was also later published by Koranne et al.[160]

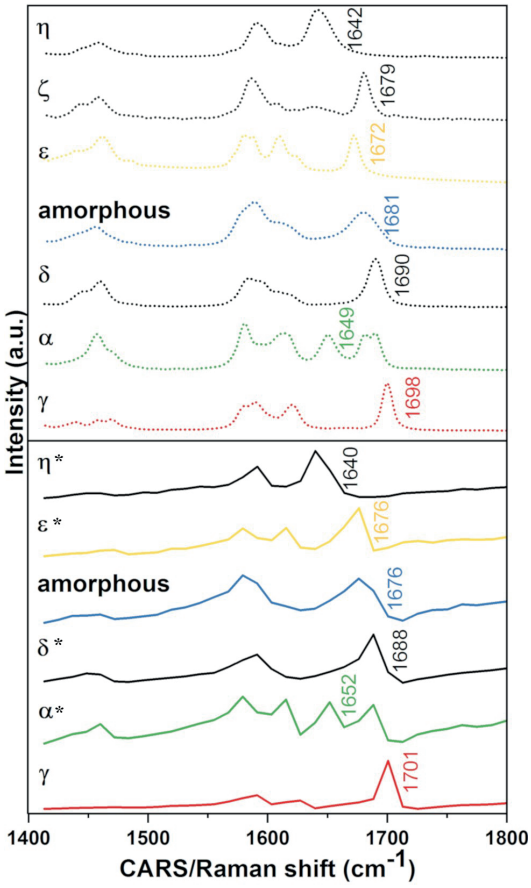

Figure 15 *Comparison of CARS (solid lines) and Raman (dotted lines) spectra of indomethacin solid-sate forms. Raman spectra (except of the ε form) are reproduced with permission from reference [1]. CARS spectral resolution is 12 cm^{-1}, while the Raman spectral resolution is 4 cm^{-1}. Polymorphs that exhibit SFG signal are marked with asterisk (*). Reprinted with permission from publication* ***III*** *(https://pubs.acs.org/doi/10.1021/acs.molpharmaceut.8b00840). Further permissions related to the material excerpted should be directed to the ACS.*

The rapid (up to video-rate) imaging and chemical specificity with CARS have earlier been exploited in monitoring distribution and solid-state changes occurring during dissolution. CARS microscopy was initially used to image drug dissolution in static[96, 109, 110] and then dynamic media by Windbergs et al.[113] and Jurna et al.[114] Later application involved *in situ* imaging with an intrinsic dissolution set up by Fussell et al.[119] In these studies, narrowband (single frequency) CARS imaging was sufficient to identify the API

and a single phase transformation (e.g. of theophylline anhydrate to monohydrate) and allowed the video-rate imaging needed for *in situ* monitoring. However, the broader CARS spectral scans over a range of frequencies (hyperspectral or broadband imaging) can identify components whose emergence otherwise cannot be predicted. For instance, broadband CARS employed by Hartshorn et al.[26] enabled detection of the unexpected formation of amorphous indomethacin upon tablet compression of the crystalline γ form. In our study, hyperspectral imaging revealed up to four polymorphs, including the unexpected η form, which were often present in trace amounts.

5.3.2 Influence of coatings

As one of the most important pharmaceutical CQAs, the dissolution performance of polymer-stabilized samples was tested. Dissolution of PVP-coated amorphous indomethacin compacts in phosphate buffer at pH 6.8 was assessed in correlation with stability studies at 30°C/75%RH. In general, PVP-coatings maintained the intrinsic dissolution rates (IDR) of fresh amorphous indomethacin (day 0 sample) in the initial stages of dissolution, despite the short-term storage that preceded the testing (**Figure 16**). This effect was present regardless of the coating thickness, however, samples coated with ten spray cycles (around 1 μm thick) showed a decrease in IDRs sooner than samples with the thinner coating (around 200 nm). Dissolution in the early stages of dissolution mainly depended on the storage time and the extent of crystallinity present prior to dissolution. However, even though the initial IDRs were equal to that of the uncoated amorphous indomethacin, after approximately five to ten minutes the IDRs started to decrease, indicating a solution-mediated solid-state transformation. In addition, some coating layer thickness-dependent trends in dissolution profiles could be observed at this stage as well. For instance, samples with the thicker coating had dissolution profiles with concentrations below that of the crystalline α form of indomethacin in the latter stages of dissolution. The presence of polymer affected the dissolution primarily in these later stages, and the observed coating thickness dependent differences are likely caused by several factors, including increased concentration of the polymer at the dissolving surface, preventing nucleation and crystal growth (recrystallization from the solution) more strongly with the thicker coatings.

This coating method has been used for the first time to coat amorphous samples. The study showed that even very thin coatings, and differences in coating thickness, can influence crystallization and dissolution behavior. In the future, it would be worth investigating this approach further with other drugs, polymers (or other coating agents such as lipids) and coating thicknesses to determine how generalizable these findings are.

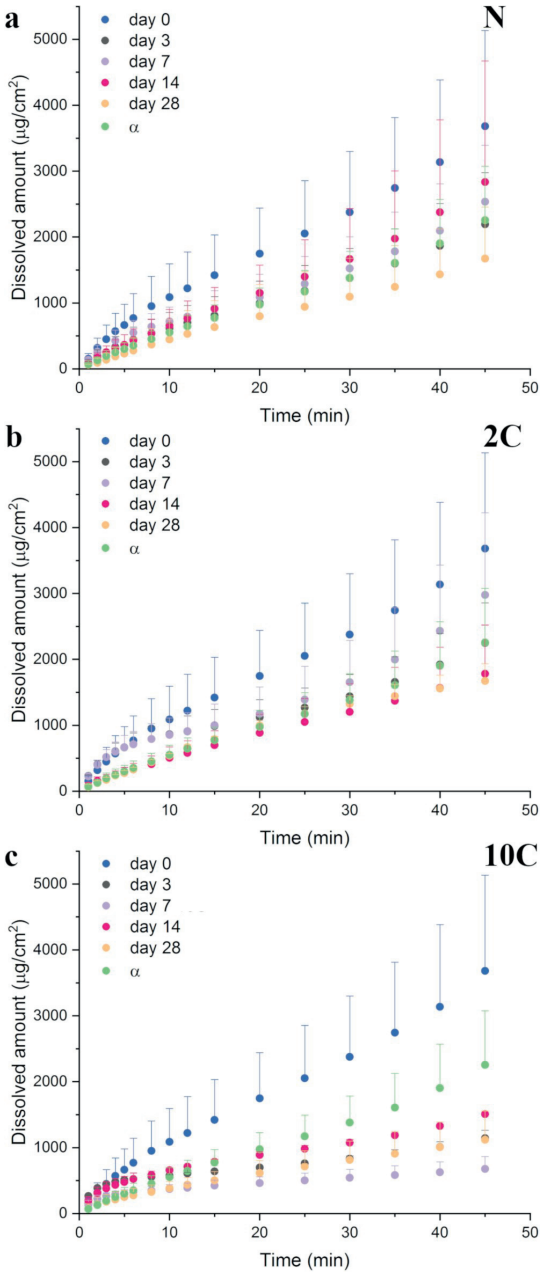

Figure 16 *Intrinsic dissolution profiles in phosphate buffer at pH 6.8 of a) uncoated versus PVP-coated b) with two spraying cycles (2C) and c) with ten spraying cycles (10C) amorphous indomethacin compacts stored at 30°C/75%RH.*

6 Conclusions

The overall aim of this thesis was to utilize relatively novel, surface specific nonlinear imaging techniques to aid understanding of solid-state behavior at the surfaces of drug particles and tablets. This understanding established the importance of surfaces in compression-, storage- and dissolution-induced crystallization and the benefits of surface- and solid-state sensitive techniques in the study of surface phenomena. Moreover, surface versus bulk behavior was discriminated and the surface stabilized with thin polymer coatings.

Firstly, surface and solid-state specific imaging methods able to differentiate multiple solid state forms were established. SFG imaging proved to be a very sensitive tool in monitoring low levels of surface crystallization; however, it is in principle limited to single phase-transitions in which the absence or presence of SFG signal is a sufficient differentiator. On the other hand, multimodal nonlinear imaging (combination of SFG and CARS) can be used to simultaneously monitor multiple solid-state forms and their phase transformations. The combination of the two techniques relying on different mechanisms (SFG – detection of noncentrosymmetric crystals and CARS – detection of molecular vibrations) was used for the first time in pharmaceutical samples. It was shown that the narrowband imaging can provide fast analysis of known samples, whereas the more time-consuming hyperspectral imaging can be used for analysis of complex pharmaceutical mixtures, which can contain unexpected components or solid-state forms.

Nonlinear imaging approaches established in first part of the work were found to be very suitable for all later studied applications – monitoring of compression, storage and dissolution induced crystallization. Moreover, the PCA method developed for hyperspectral CARS imaging was utilized in a subsequent study for monitoring the crystallization of multicomponent tablets. As this work involved the use of a commercially available fully integrated microscope, it is likely that further studies of pharmaceutical applications will follow.

Secondly, imaging approach established in the first part of the thesis was used to compare surface and bulk crystallization, as well as to monitor physical stability of neat amorphous drugs and the effect of excipients on drugs' stability during storage. Both the SFG imaging of surface versus bulk crystallization in compressed powders, as well as the SEM cross section images of continuous particle tablets confirmed that the crystallization was surface-biased. Physical mixtures of amorphous drug and polymer excipients were shown to have a varying effect on the extent of bulk crystallinity, which is of overall importance for development of amorphous formulations, but were overall inefficient in lowering or preventing surface crystallization. In contrast, thin polymer coatings (hundreds of nanometers and a micrometer thick) can delay the onset of surface crystallization during storage at high humidity. Furthermore, this effect was dependent on the coating thickness.

Thirdly, the effect of storage-induced solid-state changes on dissolution performance of neat and polymer-stabilized amorphous drugs was assessed. It was shown that early-stage storage-induced surface crystallization, undetectable by conventional solid-state analysis methods, does not necessarily impair the dissolution performance of amorphous materials, although further studies with other model drugs are needed to confirm the generalizability

of this finding. Rather, the performance was reduced only in later stages of storage, when surface crystallinity was more wide-spread. When assessing the dissolution behavior, both the solid-state prior to dissolution testing and solution-mediated transformations and crystallization occurring during the dissolution should be considered. Both the decrease in the dissolution rate due to crystallization and increase due to potentially more-soluble metastable polymorphs and changes in surface-area affect the final performance. Surface-specific, spatially resolved and solid-state specific multimodal nonlinear imaging is a highly suitable tool for providing insights into these phenomena.

The physical stabilization achieved with polymer coatings does not necessarily improve the dissolution rate of the amorphous drug form. Rather, a more thorough understanding of other properties of excipient polymers such as their concentration and viscosity effects have to be taken into account. This is particularly true when the aim is to achieve both the physical stabilization and dissolution rate maintenance or improvement during the shelf life of amorphous formulations. Further studies with other model drugs and stabilizers are needed.

All imaging strategies used in this thesis are expected to be more broadly applied in pharmaceutical industry, academia and regulatory agencies in the future. SFG and narrowband CARS imaging would be mostly suitable for fast, sensitive and non-destructive analysis for quality control purposes while the full potential of hyperspectral CARS and multimodal nonlinear imaging could be very insightful in research and development. Future applications of CARS imaging in pharmaceutics will likely include exploration of the possibilities for quantitative analysis, despite the difficulties posed by the presence of the non-linear response to concentration, including a non-resonant background signal. Addition of SRS possibilities within the same instrument capable of simultaneous SFG, CARS and TPEF imaging is already possible, and thus different nonlinear techniques can be even further combined. In addition, further developments of data processing for generating and analyzing of hyperspectral images such as with multivariate analysis are to be expected. Together with the growing number of commercially available instruments, this will make nonlinear imaging methods much more widely used in the future.

There is a growing focus on the importance of surface phenomena in pharmaceuticals, such as surface crystallization and its prevention for the amorphous drug form. In the future, an increase in the demand and analytical developments for the surface specific solid-state analysis can be expected, as it is becoming increasingly evident that the surface properties govern pharmaceutical performance. Overall, as this thesis has shown, the superficial interactions are not that superficial after all.

References

1. Surwase, S. A.; Boetker, J. P.; Saville, D.; Boyd, B. J.; Gordon, K. C.; Peltonen, L.; Strachan, C. J. Indomethacin: New polymorphs of an old drug. *Mol. Pharm.* **2013,** *10*, (12), 4472-4480.
2. Reflection paper on the use of cocrystals of active substances in medicinal products. European Medicines Agency: London, 2015.
3. Healy, A. M.; Worku, Z. A.; Kumar, D.; Madi, A. M. Pharmaceutical solvates, hydrates and amorphous forms: A special emphasis on cocrystals. *Adv. Drug Deliv. Rev.* **2017,** *117*, 25-46.
4. Lipinski, C. A. Drug-like properties and the causes of poor solubility and poor permeability. *J. Pharmacol. Toxicol. Methods* **2000,** *44*, (1), 235-249.
5. Gardner, C. R.; Walsh, C. T.; Almarsson, Ö. Drugs as materials: valuing physical form in drug discovery. *Nat. Rev. Drug Discov.* **2004,** *3*, (11), 926-934.
6. Hancock, B. C.; Zografi, G. Characteristics and significance of the amorphous state in pharmaceutical systems. *J. Pharm. Sci.* **1997,** *86*, (1), 1-12.
7. Aaltonen, J.; Allesø, M.; Mirza, S.; Koradia, V.; Gordon, K. C.; Rantanen, J. Solid form screening – A review. *Eur. J. Pharm. Biopharm.* **2009,** *71*, (1), 23-37.
8. Gaisford, S.; Saunders, M., *Essentials of pharmaceutical preformulation*. First ed.; John Whiley & Sons, Ltd.: **2013**.
9. Massa, W., *Crystal structure determination*. Second ed.; Springer: 2004.
10. Donahue Michael; Botonjic-Sehic Edita; Wells David; Chris, B. W. Understanding infrared and Raman spectra of pharmaceutical polymorphs. *Am Pharmaceut Rev* **2011**.
11. Amidon, G. L.; Lennernäs, H.; Shah, V. P.; Crison, J. R. A theoretical basis for a biopharmaceutic drug classification: The correlation of in vitro drug product dissolution and in vivo bioavailability. *Pharm. Res.* **1995,** *12*, (3), 413-420.
12. Guideline on the investigation of bioequivalence. European Medicines Agency: London, 2010.
13. Murdande, S. B.; Pikal, M. J.; Shanker, R. M.; Bogner, R. H. Solubility advantage of amorphous pharmaceuticals: I. A thermodynamic analysis. *J. Pharm. Sci.* **2010,** *99*, (3), 1254-1264.
14. Hancock, B. C.; Parks, M. What is the true solubility advantage for amorphous pharmaceuticals? *Pharm. Res.* **2000,** *17*, (4), 397-404.
15. Strachan, C. J.; Rades, T.; Gordon, K. C. A theoretical and spectroscopic study of γ-crystalline and amorphous indometacin. *J. Pharm. Pharmacol.* **2007,** *59*, (2), 261-269.
16. Hancock, B. C.; Shalaev, E. Y.; Shamblin, S. L. Polyamorphism: a pharmaceutical science perspective. *J. Pharm. Pharmacol.* **2002,** *54*, (8), 1151-1152.
17. Karmwar, P.; Graeser, K.; Gordon, K. C.; Strachan, C. J.; Rades, T. Investigation of properties and recrystallisation behaviour of amorphous indomethacin samples prepared by different methods. *Int. J. Pharm.* **2011,** *417*, (1-2), 94-100.
18. Karmwar, P.; Graeser, K.; Gordon, K. C.; Strachan, C. J.; Rades, T. Effect of different preparation methods on the dissolution behaviour of amorphous indomethacin. *Eur. J. Pharm. Biopharm.* **2012,** *80*, (2), 459-464.
19. Rades, T.; Gordon, K. C.; Graeser, K., Molecular structure, properties and states of matter. In *Remington - Essentials of pharmaceutics*, Pharmaceutical Press.
20. Yu, L. Amorphous pharmaceutical solids: preparation, characterization and stabilization. *Adv. Drug Deliv. Rev.* **2001,** *48*, (1), 27-42.
21. Kissi, E. O.; Grohganz, H.; Löbmann, K.; Ruggiero, M. T.; Zeitler, J. A.; Rades, T. Glass-transition temperature of the β-relaxation as the major predictive parameter for recrystallization of neat amorphous drugs. *J. Phys. Chem. B* **2018,** *122*, (10), 2803-2808.
22. Heinz, A.; Strachan, C. J.; Gordon, K. C.; Rades, T. Analysis of solid-state transformations of pharmaceutical compounds using vibrational spectroscopy. *J. Pharm. Pharmacol.* **2009,** *61*, (8), 971-988.

23. Tuschel, D. Why are the Raman spectra of crystalline and amorphous solids different? *Spectroscopy* **2017,** *32*, (3), 26-33.
24. Yoshioka, M.; Hancock, B. C.; Zografi, G. Crystallization of indomethacin from the amorphous state below and above its glass transition temperature. *J. Pharm. Sci.* **1994,** *83*, (12), 1700-1705.
25. Yu, L. Surface mobility of molecular glasses and its importance in physical stability. *Adv. Drug Deliv. Rev.* **2016,** *100*, 3-9.
26. Hartshorn, C. M.; Lee, Y. J.; Camp, C. H.; Liu, Z.; Heddleston, J.; Canfield, N.; Rhodes, T. A.; Hight Walker, A. R.; Marsac, P. J.; Cicerone, M. T. Multicomponent chemical imaging of pharmaceutical solid dosage forms with broadband CARS microscopy. *Anal. Chem.* **2013,** *85*, (17), 8102-8111.
27. Debnath, S.; Suryanarayanan, R. Influence of processing-induced phase transformations on the dissolution of theophylline tablets. *AAPS PharmSciTech* **2009,** *5*, (1), 39.
28. Hancock, B. C.; Zografi, G. The relationship between the glass transition temperature and the water content of amorphous pharmaceutical solids. *Pharm. Res.* **1994,** *11*, (4), 471-477.
29. Thakral, N. K.; Mohapatra, S.; Stephenson, G. A.; Suryanarayanan, R. Compression-induced crystallization of amorphous indomethacin in tablets: Characterization of spatial heterogeneity by two-dimensional X-ray diffractometry. *Mol. Pharm.* **2015,** *12*, (1), 253-263.
30. Bērziņš, K. r.; Fraser-Miller, S. J.; Rades, T.; Gordon, K. C. Low-frequency Raman spectroscopic study on compression-induced destabilization in melt-quenched amorphous celecoxib. *Mol. Pharm.* **2019,** *16*, (8), 3678-3686.
31. Andronis, V.; Yoshioka, M.; Zografi, G. Effects of sorbed water on the crystallization of indomethacin from the amorphous state. *J. Pharm. Sci.* **1997,** *86*, (3), 346-351.
32. Shi, Q.; Zhang, C.; Su, Y.; Zhang, J.; Zhou, D.; Cai, T. Acceleration of crystal growth of amorphous griseofulvin by low-concentration poly(ethylene oxide): Aspects of crystallization kinetics and molecular mobility. *Mol. Pharm.* **2017,** *14*, (7), 2262-2272.
33. Powell, C. T.; Cai, T.; Hasebe, M.; Gunn, E. M.; Gao, P.; Zhang, G.; Gong, Y.; Yu, L. Low-concentration polymers inhibit and accelerate crystal growth in organic glasses in correlation with segmental mobility. *J. Phys. Chem. B* **2013,** *117*, (35), 10334-10341.
34. Hsu, H.-Y.; Harris, M. T.; Toth, S.; Simpson, G. J. Drop printing of pharmaceuticals: Effect of molecular weight on PEG coated-naproxen/PEG 3350 solid dispersions. *AIChE J.* **2015,** *61*, (12), 4502-4508.
35. Crowley, K. J.; Zografi, G. The effect of low concentrations of molecularly dispersed poly(vinylpyrrolidone) on indomethacin crystallization from the amorphous state. *Pharm. Res.* **2003,** *20*, (9), 1417-1422.
36. Imaizumi, H.; Nambu, N.; Nagai, T. Stabilization of amorphous state of indomethacin by solid dispersion in polyvinylpolypyrrolidone. *Chem. Pharm. Bull. (Tokyo)* **1983,** *31*, (7), 2510-2512.
37. Wu, T.; Yu, L. Surface crystallization of indomethacin below T_g. *Pharm. Res.* **2006,** *23*, (10), 2350-2355.
38. Zhu, L.; Jona, J.; Nagapudi, K.; Wu, T. Fast surface crystallization of amorphous griseofulvin below T_g. *Pharm. Res.* **2010,** *27*, (8), 1558-1567.
39. Kestur, U. S.; Ivanesivic, I.; Alonzo, D. E.; Taylor, L. S. Influence of particle size on the crystallization kinetics of amorphous felodipine powders. *Powder Technol.* **2013,** *236*, 197-204.
40. Zhu, L.; Wong, L.; Yu, L. Surface-enhanced crystallization of amorphous nifedipine. *Mol. Pharm.* **2008,** *5*, (6), 921-926.
41. Zeng, A.; Yao, X.; Gui, Y.; Li, Y.; Jones, K. J.; Yu, L. Inhibiting surface crystallization and improving dissolution of amorphous loratadine by dextran sulfate nanocoating. *J. Pharm. Sci.* **2019,** *108*, (7), 2391-2396.

42. Gui, Y.; Chen, Y.; Chen, Z.; Jones, K. J.; Yu, L. Improving stability and dissolution of amorphous clofazimine by polymer nano-coating. *Pharm. Res.* **2019,** *36*, (5), 67.
43. Shi, Q.; Cai, T. Fast crystal growth of amorphous griseofulvin: Relations between bulk and surface growth modes. *Cryst. Growth Des.* **2016,** *16*, (6), 3279-3286.
44. Kestur, U. S.; Taylor, L. S. Evaluation of the crystal growth rate of felodipine polymorphs in the presence and absence of additives as a function of temperature. *Cryst. Growth Des.* **2013,** *13*, (10), 4349-4354.
45. Sun, Y.; Zhu, L.; Wu, T.; Cai, T.; Gunn, E. M.; Yu, L. Stability of amorphous pharmaceutical solids: Crystal growth mechanisms and effect of polymer additives. *AAPS J.* **2012,** *14*, (3), 380-388.
46. Sun, Y.; Zhu, L.; Kearns, K. L.; Ediger, M. D.; Yu, L. Glasses crystallize rapidly at free surfaces by growing crystals upward. *Proc. Natl. Acad. Sci. U. S. A.* **2011,** *108*, (15), 5990-5995.
47. Cai, T.; Zhu, L.; Yu, L. Crystallization of organic glasses: Effects of polymer additives on bulk and surface crystal growth in amorphous nifedipine. *Pharm. Res.* **2011,** *28*, (10), 2458-2466.
48. Hasebe, M.; Musumeci, D.; Yu, L. Fast surface crystallization of molecular glasses: Creation of depletion zones by surface diffusion and crystallization flux. *J. Phys. Chem. B* **2015,** *119*, (7), 3304-3311.
49. Zhu, L.; Brian, C. W.; Swallen, S. F.; Straus, P. T.; Ediger, M. D.; Yu, L. Surface self-diffusion of an organic glass. *Phys. Rev. Lett.* **2011,** *106*, (25), 256103.
50. Huang, C.; Ruan, S.; Cai, T.; Yu, L. Fast surface diffusion and crystallization of amorphous griseofulvin. *J. Phys. Chem. B* **2017,** *121*, (40), 9463-9468.
51. Brian, C. W.; Yu, L. Surface self-diffusion of organic glasses. *J. Phys. Chem. A* **2013,** *117*, (50), 13303-13309.
52. Wu, T.; Sun, Y.; Li, N.; de Villiers, M. M.; Yu, L. Inhibiting surface crystallization of amorphous indomethacin by nanocoating. *Langmuir* **2007,** *23*, (9), 5148-5153.
53. Ng, Y. C.; Yang, Z.; McAuley, W. J.; Qi, S. Stabilisation of amorphous drugs under high humidity using pharmaceutical thin films. *Eur. J. Pharm. Biopharm.* **2013,** *84*, (3), 555-565.
54. Capece, M.; Davé, R. Enhanced physical stability of amorphous drug formulations via dry polymer coating. *J. Pharm. Sci.* **2015,** *104*, (6), 2076-2084.
55. Teerakapibal, R.; Gui, Y.; Yu, L. Gelatin nano-coating for inhibiting surface crystallization of amorphous drugs. *Pharm. Res.* **2018,** *35*, (1), 23.
56. Powell, C. T.; Xi, H.; Sun, Y.; Gunn, E.; Chen, Y.; Ediger, M. D.; Yu, L. Fast crystal growth in o-terphenyl glasses: A possible role for fracture and surface mobility. *J. Phys. Chem. B* **2015,** *119*, (31), 10124-10130.
57. Vasconcelos, T.; Sarmento, B.; Costa, P. Solid dispersions as strategy to improve oral bioavailability of poor water soluble drugs. *Drug Discovery Today* **2007,** *12*, (23), 1068-1075.
58. Qi, S.; McAuley, W. J.; Yang, Z.; Tipduangta, P. Physical stabilization of low-molecular-weight amorphous drugs in the solid state: a material science approach. *Ther. Deliv.* **2014,** *5*, (7), 817-841.
59. Terife, G.; Wang, P.; Faridi, N.; Gogos, C. G. Hot melt mixing and foaming of Soluplus® and indomethacin. *Polym. Eng. Sci.* **2012,** *52*, (8), 1629-1639.
60. Taylor, L. S.; Zografi, G. Spectroscopic characterization of interactions between PVP and indomethacin in amorphous molecular dispersions. *Pharm. Res.* **1997,** *14*, (12), 1691-1698.
61. Liu, H.; Zhang, X.; Suwardie, H.; Wang, P.; Gogos, C. G. Miscibility studies of indomethacin and Eudragit® E PO by thermal, rheological, and spectroscopic analysis. *J. Pharm. Sci.* **2012,** *101*, (6), 2204-2212.
62. Mistry, P.; Mohapatra, S.; Gopinath, T.; Vogt, F. G.; Suryanarayanan, R. Role of the strength of drug–polymer interactions on the molecular mobility and crystallization inhibition in ketoconazole solid dispersions. *Mol. Pharm.* **2015,** *12*, (9), 3339-3350.

63. Van den Mooter, G. The use of amorphous solid dispersions: A formulation strategy to overcome poor solubility and dissolution rate. *Drug Discovery Today: Technologies* **2012,** *9*, (2), e79-e85.
64. Dengale, S. J.; Grohganz, H.; Rades, T.; Löbmann, K. Recent advances in co-amorphous drug formulations. *Adv. Drug Deliv. Rev.* **2016,** *100*, 116-125.
65. Luebbert, C.; Klanke, C.; Sadowski, G. Investigating phase separation in amorphous solid dispersions via Raman mapping. *Int. J. Pharm.* **2018,** *535*, (1), 245-252.
66. Laitinen, R.; Löbmann, K.; Strachan, C. J.; Grohganz, H.; Rades, T. Emerging trends in the stabilization of amorphous drugs. *Int. J. Pharm.* **2013,** *453*, (1), 65-79.
67. Lu, Q.; Zografi, G. Phase behavior of binary and ternary amorphous mixtures containing indomethacin, citric acid, and PVP. *Pharm. Res.* **1998,** *15*, (8), 1202-1206.
68. Hoppu, P.; Hietala, S.; Schantz, S.; Juppo, A. M. Rheology and molecular mobility of amorphous blends of citric acid and paracetamol. *Eur. J. Pharm. Biopharm.* **2009,** *71*, (1), 55-63.
69. Löbmann, K.; Jensen, K. T.; Laitinen, R.; Rades, T.; Strachan, C. J.; Grohganz, H., Stabilized amorphous solid dispersions with small molecule excipients. In *Amorphous Solid Dispersions: Theory and Practice*, Shah, N.; Sandhu, H.; Choi, D. S.; Chokshi, H.; Malick, A. W., Eds. Springer New York: New York, NY, 2014; pp 613-636.
70. Fussell, A. L.; Mah, P. T.; Offerhaus, H.; Niemi, S.-M.; Salonen, J.; Santos, H. A.; Strachan, C. Coherent anti-Stokes Raman scattering microscopy driving the future of loaded mesoporous silica imaging. *Acta Biomater.* **2014,** *10*, (11), 4870-4877.
71. Qian, K. K.; Bogner, R. H. Application of mesoporous silicon dioxide and silicate in oral amorphous drug delivery systems. *J. Pharm. Sci.* **2012,** *101*, (2), 444-463.
72. Santos, H. A.; Salonen, J.; Bimbo, L. M.; Lehto, V. P.; Peltonen, L.; Hirvonen, J. Mesoporous materials as controlled drug delivery formulations. *J. Drug Deliv. Sci. Technol.* **2011,** *21*, (2), 139-155.
73. Song, S. W.; Hidajat, K.; Kawi, S. Functionalized SBA-15 materials as carriers for controlled drug delivery: Influence of surface properties on matrix−drug interactions. *Langmuir* **2005,** *21*, (21), 9568-9575.
74. Li, Y.; Yu, J.; Hu, S.; Chen, Z.; Sacchetti, M.; Sun, C. C.; Yu, L. Polymer nanocoating of amorphous drugs for improving stability, dissolution, powder flow, and tabletability: The case of chitosan-coated indomethacin. *Mol. Pharm.* **2019,** *16*, (3), 1305-1311.
75. Priemel, P. A.; Laitinen, R.; Barthold, S.; Grohganz, H.; Lehto, V.-P.; Rades, T.; Strachan, C. J. Inhibition of surface crystallisation of amorphous indomethacin particles in physical drug–polymer mixtures. *Int. J. Pharm.* **2013,** *456*, (2), 301-306.
76. Fraser-Miller, S. J.; Saarinen, J.; Strachan, C. J., Vibrational spectroscopic imaging. In *Analytical Techniques in the Pharmaceutical Sciences*, Müllertz, A.; Perrie, Y.; Rades, T., Eds. Springer New York: New York, NY, 2016; pp 523-589.
77. Priemel, P. A.; Grohganz, H.; Gordon, K. C.; Rades, T.; Strachan, C. J. The impact of surface- and nano-crystallisation on the detected amorphous content and the dissolution behaviour of amorphous indomethacin. *Eur. J. Pharm. Biopharm.* **2012,** *82*, (1), 187-193.
78. Ewing, A. V.; Clarke, G. S.; Kazarian, S. G. Stability of indomethacin with relevance to the release from amorphous solid dispersions studied with ATR-FTIR spectroscopic imaging. *Eur. J. Pharm. Sci.* **2014,** *60*, 64-71.
79. Everall, N. J. Modeling and measuring the effect of refraction on the depth resolution of confocal Raman microscopy. *Appl. Spectrosc.* **2000,** *54*, (6), 773-782.
80. Parratt, L. G. Surface studies of solids by total reflection of X-rays. *Phys. Rev.* **1954,** *95*, (2), 359-369.
81. Debnath, S.; Predecki, P.; Suryanarayanan, R. Use of glancing angle X-ray powder diffractometry to depth-profile phase transformations during dissolution of indomethacin and theophylline tablets. *Pharm. Res.* **2004,** *21*, (1), 149-159.
82. Koradia, V.; Tenho, M.; Lopez de Diego, H.; Ringkjøbing-Elema, M.; Møller-Sonnergaard, J.; Salonen, J.; Lehto, V.-P.; Rantanen, J. Investigation of solid phase

composition on tablet surfaces by grazing incidence X-ray diffraction. *Pharm. Res.* **2012,** *29*, (1), 134-144.
83. Prats-Mateu, B.; Gierlinger, N. Tip in–light on: Advantages, challenges, and applications of combining AFM and Raman microscopy on biological samples. *Microsc. Res. Tech.* **2017,** *80*, (1), 30-40.
84. Bailo, E.; Deckert, V. Tip-enhanced Raman scattering. *Chem. Soc. Rev.* **2008,** *37*, (5), 921-930.
85. Zeitler, J. A., Pharmaceutical terahertz spectroscopy and imaging. In *Analytical techniques in the pharmaceutical sciences*, Springer.
86. Ho, L.; Müller, R.; Krüger, C.; Gordon, K. C.; Kleinebudde, P.; Pepper, M.; Rades, T.; Shen, Y.; Taday, P. F.; Zeitler, J. A. Investigating dissolution performance critical areas on coated tablets: A case study using terahertz pulsed imaging. *J. Pharm. Sci.* **2010,** *99*, (1), 392-402.
87. Kempson, I. M.; Prestidge, C. A., Mass spectrometry imaging of pharmaceuticals: from tablets to tissues. In *Analytical techniques in the pharmaceutical sciences*, Springer: 2016.
88. Barnes, T. J.; Kempson, I. M.; Prestidge, C. A. Surface analysis for compositional, chemical and structural imaging in pharmaceutics with mass spectrometry: A ToF-SIMS perspective. *Int. J. Pharm.* **2011,** *417*, (1), 61-69.
89. Belu, A.; Mahoney, C.; Wormuth, K. Chemical imaging of drug eluting coatings: Combining surface analysis and confocal Raman microscopy. *J. Control. Release* **2008,** *126*, (2), 111-121.
90. Prestidge, C. A.; Barnes, T. J.; Skinner, W. Time-of-flight secondary-ion mass spectrometry for the surface characterization of solid-state pharmaceuticals. *J. Pharm. Pharmacol.* **2007,** *59*, (2), 251-259.
91. Strachan, C. J.; Taday, P. F.; Newnham, D. A.; Gordon, K. C.; Zeitler, J. A.; Pepper, M.; Rades, T. Using terahertz pulsed spectroscopy to quantify pharmaceutical polymorphism and crystallinity. *J. Pharm. Sci.* **2005,** *94*, (4), 837-846.
92. Schneider, L.; Peukert, W. Second harmonic generation spectroscopy as a method for in situ and online characterization of particle surface properties. *Part. Part. Syst. Char.* **2006,** *23*, (5), 351-359.
93. Strachan, C. J.; Windbergs, M.; Offerhaus, H. L. Pharmaceutical applications of non-linear imaging. *Int. J. Pharm.* **2011,** *417*, (1), 163-172.
94. Boyd, R., *Nonlinear optics*. Third ed.; Academic Press Burlington, 2008.
95. Zumbusch, A.; Holtom, G. R.; Xie, X. S. Three-dimensional vibrational imaging by coherent anti-Stokes Raman scattering. *Phys. Rev. Lett.* **1999,** *82*, (20), 4142-4145.
96. Kang, E.; Wang, H.; Kwon, I. K.; Robinson, J.; Park, K.; Cheng, J.-X. In situ visualization of paclitaxel distribution and release by coherent anti-Stokes Raman scattering microscopy. *Anal. Chem.* **2006,** *78*, (23), 8036-8043.
97. Strachan, C. J.; Lee, C. J.; Rades, T. Partial characterization of different mixtures of solids by measuring the optical nonlinear response. *J. Pharm. Sci.* **2004,** *93*, (3), 733-742.
98. Kestur, U. S.; Wanapun, D.; Toth, S. J.; Wegiel, L. A.; Simpson, G. J.; Taylor, L. S. Nonlinear optical imaging for sensitive detection of crystals in bulk amorphous powders. *J. Pharm. Sci.* **2012,** *101*, (11), 4201-4213.
99. Wanapun, D.; Kestur, U. S.; Taylor, L. S.; Simpson, G. J. Single particle nonlinear optical imaging of trace crystallinity in an organic powder. *Anal. Chem.* **2011,** *83*, (12), 4745-4751.
100. Schmitt, P. D.; Trasi, N. S.; Taylor, L. S.; Simpson, G. J. Finding the needle in the haystack: Characterization of trace crystallinity in a commercial formulation of paclitaxel protein-bound particles by Raman spectroscopy enabled by second harmonic generation microscopy. *Mol. Pharm.* **2015,** *12*, (7), 2378-2383.
101. Song, Z.; Sarkar, S.; Vogt, A. D.; Danzer, G. D.; Smith, C. J.; Gualtieri, E. J.; Simpson, G. J. Kinetic modeling of accelerated stability testing enabled by second harmonic generation microscopy. *Anal. Chem.* **2018,** *90*, (7), 4406-4413.

102. Franken, P. A.; Hill, A. E.; Peters, C. W.; Weinreich, G. Generation of optical harmonics. *Phys. Rev. Lett.* **1961,** *7*, (4), 118-119.
103. Maker, P. D.; Terhune, R. W. Study of optical effects due to an induced polarization third order in the electric field strength. *Phys. Rev.* **1965,** *137*, (3A), A801-A818.
104. Slipchenko, M. N.; Chen, H.; Ely, D. R.; Jung, Y.; Carvajal, M. T.; Cheng, J.-X. Vibrational imaging of tablets by epi-detected stimulated Raman scattering microscopy. *Analyst* **2010,** *135*, (10), 2613-2619.
105. Schmitt, P. D. Recent advances in nonlinear optical analyses of pharmaceutical materials in the solid state. *Mol. Pharm.* **2017,** *14*, (3), 555-565.
106. Lee, C. J.; Strachan, C. J.; Manson, P. J.; Rades, T. Characterization of the bulk properties of pharmaceutical solids using nonlinear optics - a review. *J. Pharm. Pharmacol.* **2007,** *59*, (2), 241-250.
107. Evans, C. L.; Xie, X. S. Coherent anti-Stokes Raman scattering microscopy: Chemical imaging for biology and medicine. *Annu. Rev. Anal. Chem. (Palo Alto Calif.)* **2008,** *1*, (1), 883-909.
108. Pautot, S.; Frisken, B. J.; Cheng, J.-X.; Xie, X. S.; Weitz, D. A. Spontaneous formation of lipid structures at oil/water/lipid interfaces. *Langmuir* **2003,** *19*, (24), 10281-10287.
109. Kang, E.; Robinson, J.; Park, K.; Cheng, J.-X. Paclitaxel distribution in poly(ethylene glycol)/poly(lactide-co-glycolic acid) blends and its release visualized by coherent anti-Stokes Raman scattering microscopy. *J. Control. Release* **2007,** *122*, (3), 261-268.
110. Kang, E.; Wang, H.; Kwon, I. K.; Song, Y.-H.; Kamath, K.; Miller, K. M.; Barry, J.; Cheng, J.-X.; Park, K. Application of coherent anti-stokes Raman scattering microscopy to image the changes in a paclitaxel–poly(styrene-b-isobutylene-b-styrene) matrix pre- and post-drug elution. *J. Biomed. Mater. Res.* **2008,** *87A*, (4), 913-920.
111. Fussell, A.; Isomäki, A.; Strachan, C. Nonlinear optical imaging – introduction and pharmaceutical applications. *Am Pharmaceut Rev* **2013**.
112. Strachan, C. J.; Rades, T.; Lee, C. J. Determination of the optical second harmonic response of pharmaceutical solid–solid mixtures. *Optics and Lasers in Engineering* **2005,** *43*, (2), 209-220.
113. Windbergs, M.; Jurna, M.; Offerhaus, H. L.; Herek, J. L.; Kleinebudde, P.; Strachan, C. J. Chemical imaging of oral solid dosage forms and changes upon dissolution using coherent anti-Stokes Raman scattering microscopy. *Anal. Chem.* **2009,** *81*, (6), 2085-2091.
114. Jurna, M.; Windbergs, M.; Strachan, C. J.; Hartsuiker, L.; Otto, C.; Kleinebudde, P.; Herek, J. L.; Offerhaus, H. L. Coherent anti-Stokes Raman scattering microscopy to monitor drug dissolution in different oral pharmaceutical tablets. *Journal of Innovative Optical Health Sciences* **2009,** *2*, (1), 37-43.
115. Wanapun, D.; Kestur, U. S.; Kissick, D. J.; Simpson, G. J.; Taylor, L. S. Selective detection and quantitation of organic molecule crystallization by second harmonic generation microscopy. *Anal. Chem.* **2010,** *82*, (13), 5425-5432.
116. Toth, S. J.; Madden, J. T.; Taylor, L. S.; Marsac, P.; Simpson, G. J. Selective imaging of active pharmaceutical ingredients in powdered blends with common excipients utilizing two-photon excited ultraviolet-fluorescence and ultraviolet-second order nonlinear optical imaging of chiral crystals. *Anal. Chem.* **2012,** *84*, (14), 5869-5875.
117. Hsu, H.-Y.; Toth, S. J.; Simpson, G. J.; Taylor, L. S.; Harris, M. T. Effect of substrates on naproxen-polyvinylpyrrolidone solid dispersions formed via the drop printing technique. *J. Pharm. Sci.* **2013,** *102*, (2), 638-648.
118. Garbacik, E. T.; Korterik, J. P.; Otto, C.; Herek, J. L.; Offerhaus, H. L. Epi-detection of vibrational phase contrast coherent anti-Stokes Raman scattering. *Opt. Lett.* **2014,** *39*, (20), 5814-5817.
119. Fussell, A.; Garbacik, E.; Offerhaus, H.; Kleinebudde, P.; Strachan, C. In situ dissolution analysis using coherent anti-Stokes Raman scattering (CARS) and hyperspectral CARS microscopy. *Eur. J. Pharm. Biopharm.* **2013,** *85*, (3, Part B), 1141-1147.

120. Zhu, Q.; Toth, S. J.; Simpson, G. J.; Hsu, H.-Y.; Taylor, L. S.; Harris, M. T. Crystallization and dissolution behavior of naproxen/polyethylene glycol solid dispersions. *J. Phys. Chem. B* **2013,** *117*, (5), 1494-1500.
121. Chowdhury, A. U.; Dettmar, C. M.; Sullivan, S. Z.; Zhang, S.; Jacobs, K. T.; Kissick, D. J.; Maltais, T.; Hedderich, H. G.; Bishop, P. A.; Simpson, G. J. Kinetic trapping of metastable amino acid polymorphs. *J. Am. Chem. Soc.* **2014,** *136*, (6), 2404-2412.
122. Ghorab, M. K.; Toth, S. J.; Simpson, G. J.; Mauer, L. J.; Taylor, L. S. Water–solid interactions in amorphous maltodextrin-crystalline sucrose binary mixtures. *Pharm. Dev. Technol.* **2014,** *19*, (2), 247-256.
123. Pegoraro, A. F.; Slepkov, A. D.; Ridsdale, A.; Moffatt, D. J.; Stolow, A. Hyperspectral multimodal CARS microscopy in the fingerprint region. *Journal of Biophotonics* **2014,** *7*, (1-2), 49-58.
124. Fussell, A. L.; Grasmeijer, F.; Frijlink, H. W.; de Boer, A. H.; Offerhaus, H. L. CARS microscopy as a tool for studying the distribution of micronised drugs in adhesive mixtures for inhalation. *J. Raman Spectrosc.* **2014,** *45*, (7), 495-500.
125. DeWalt, E. L.; Sullivan, S. Z.; Schmitt, P. D.; Muir, R. D.; Simpson, G. J. Polarization-modulated second harmonic generation ellipsometric microscopy at video rate. *Anal. Chem.* **2014,** *86*, (16), 8448-8456.
126. Jackson, M. J.; Toth, S. J.; Kestur, U. S.; Huang, J.; Qian, F.; Hussain, M. A.; Simpson, G. J.; Taylor, L. S. Impact of polymers on the precipitation behavior of highly supersaturated aqueous danazol solutions. *Mol. Pharm.* **2014,** *11*, (9), 3027-3038.
127. Toth, S. J.; Schmitt, P. D.; Snyder, G. R.; Trasi, N. S.; Sullivan, S. Z.; George, I. A.; Taylor, L. S.; Simpson, G. J. Ab Initio prediction of the diversity of second harmonic generation from pharmaceutically relevant materials. *Cryst. Growth Des.* **2015,** *15*, (2), 581-586.
128. Christophersen, P. C.; Birch, D.; Saarinen, J.; Isomäki, A.; Nielsen, H. M.; Yang, M.; Strachan, C. J.; Mu, H. Investigation of protein distribution in solid lipid particles and its impact on protein release using coherent anti-Stokes Raman scattering microscopy. *J. Control. Release* **2015,** *197*, 111-120.
129. Newman, J. A.; Schmitt, P. D.; Toth, S. J.; Deng, F.; Zhang, S.; Simpson, G. J. Parts per million powder X-ray diffraction. *Anal. Chem.* **2015,** *87*, (21), 10950-10955.
130. Schmitt, P. D.; DeWalt, E. L.; Dow, X. Y.; Simpson, G. J. Rapid discrimination of polymorphic crystal forms by nonlinear optical Stokes ellipsometric microscopy. *Anal. Chem.* **2016,** *88*, (11), 5760-5768.
131. Chowdhury, A. U.; Ye, D. H.; Song, Z.; Zhang, S.; Hedderich, H. G.; Mallick, B.; Thirunahari, S.; Ramakrishnan, S.; Sengupta, A.; Gualtieri, E. J.; Bouman, C. A.; Simpson, G. J. Second harmonic generation guided Raman spectroscopy for sensitive detection of polymorph transitions. *Anal. Chem.* **2017,** *89*, (11), 5958-5965.
132. Correa-Soto, C.; Trasi, N. S.; Schmitt, P. D.; Su, Y.; Liu, Z.; Miller, E.; Variankaval, N.; Marsac, P. J.; Simpson, G. J.; Taylor, L. S. Second harmonic generation microscopy as a tool for the early detection of crystallization in spray dried dispersions. *J. Pharm. Biomed. Anal.* **2017,** *146*, 86-95.
133. Elkhabaz, A.; Sarkar, S.; Dinh, J. K.; Simpson, G. J.; Taylor, L. S. Variation in supersaturation and phase behavior of ezetimibe amorphous solid dispersions upon dissolution in different biorelevant media. *Mol. Pharm.* **2018,** *15*, (1), 193-206.
134. Ojarinta, R.; Saarinen, J.; Strachan, C. J.; Korhonen, O.; Laitinen, R. Preparation and characterization of multi-component tablets containing co-amorphous salts: Combining multimodal non-linear optical imaging with established analytical methods. *Eur. J. Pharm. Biopharm.* **2018,** *132*, 112-126.
135. Porquez, J. G.; Slepkov, A. D. Application of spectral-focusing-CARS microscopy to pharmaceutical sample analysis. *American Institute of Physics Advances* **2018,** *8*, (9), 095213.
136. Smith, C. J.; Dinh, J.; Schmitt, P. D.; Stroud, P. A.; Hinds, J.; Johnson, M. J.; Simpson, G. J. Calibration-free second harmonic generation (SHG) image analysis for quantification of trace crystallinity within final dosage forms of amorphous solid dispersions. *Appl. Spectrosc.* **2018,** *72*, (11), 1594-1605.

137. Figueroa, B.; Nguyen, T.; Sotthivirat, S.; Xu, W.; Rhodes, T.; Lamm, M. S.; Smith, R. L.; John, C. T.; Su, Y.; Fu, D. Detecting and quantifying microscale chemical reactions in pharmaceutical tablets by stimulated Raman scattering microscopy. *Anal. Chem.* **2019,** *91*, (10), 6894-6901.
138. Savolainen, M.; Kogermann, K.; Heinz, A.; Aaltonen, J.; Peltonen, L.; Strachan, C.; Yliruusi, J. Better understanding of dissolution behaviour of amorphous drugs by in situ solid-state analysis using Raman spectroscopy. *Eur. J. Pharm. Biopharm.* **2009,** *71*, (1), 71-79.
139. Strachan, C. J.; Pratiwi, D.; Gordon, K. C.; Rades, T. Quantitative analysis of polymorphic mixtures of carbamazepine by Raman spectroscopy and principal components analysis. *J. Raman Spectrosc.* **2004,** *35*, (5), 347-352.
140. Savolainen, M.; Heinz, A.; Strachan, C.; Gordon, K. C.; Yliruusi, J.; Rades, T.; Sandler, N. Screening for differences in the amorphous state of indomethacin using multivariate visualization. *Eur. J. Pharm. Sci.* **2007,** *30*, (2), 113-123.
141. Guidance for industry Q8(R2) pharmaceutical development U.S Department of Health and Human Services, Food and Drug Administration (FDA): 2009.
142. Yu, L. X.; Amidon, G.; Khan, M. A.; Hoag, S. W.; Polli, J.; Raju, G. K.; Woodcock, J. Understanding pharmaceutical quality by design. *AAPS J.* **2014,** *16*, (4), 771-783.
143. Hancock, B. C.; Shamblin, S. L.; Zografi, G. Molecular mobility of amorphous pharmaceutical solids below their glass transition temperatures. *Pharm. Res.* **1995,** *12*, (6), 799-806.
144. Ruggiero, M. T.; Krynski, M.; Kissi, E. O.; Sibik, J.; Markl, D.; Tan, N. Y.; Arslanov, D.; van der Zande, W.; Redlich, B.; Korter, T. M.; Grohganz, H.; Löbmann, K.; Rades, T.; Elliott, S. R.; Zeitler, J. A. The significance of the amorphous potential energy landscape for dictating glassy dynamics and driving solid-state crystallisation. *Phys. Chem. Chem. Phys.* **2017,** *19*, (44), 30039-30047.
145. Okamoto, N.; Oguni, M. Discovery of crystal nucleation proceeding much below the glass transition temperature in a supercooled liquid. *Solid State Commun.* **1996,** *99*, (1), 53-56.
146. Bhattacharya, S.; Suryanarayanan, R. Local mobility in amorphous pharmaceuticals—characterization and implications on stability. *J. Pharm. Sci.* **2009,** *98*, (9), 2935-2953.
147. Fitzpatrick, S.; McCabe, J. F.; Petts, C. R.; Booth, S. W. Effect of moisture on polyvinylpyrrolidone in accelerated stability testing. *Int. J. Pharm.* **2002,** *246*, (1), 143-151.
148. Bhattacharya, S.; Sharma, D. K.; Saurabh, S.; De, S.; Sain, A.; Nandi, A.; Chowdhury, A. Plasticization of poly(vinylpyrrolidone) thin films under ambient humidity: Insight from single-molecule tracer diffusion dynamics. *J. Phys. Chem. B* **2013,** *117*, (25), 7771-7782.
149. Alonzo, D. E.; Zhang, G. G. Z.; Zhou, D.; Gao, Y.; Taylor, L. S. Understanding the behavior of amorphous pharmaceutical systems during dissolution. *Pharm. Res.* **2010,** *27*, (4), 608-618.
150. Greco, K.; Bogner, R. Crystallization of amorphous indomethacin during dissolution: Effect of processing and annealing. *Mol. Pharm.* **2010,** *7*, (5), 1406-1418.
151. Greco, K.; Bogner, R. Solution-mediated phase transformation: Significance during dissolution and implications for bioavailability. *J. Pharm. Sci.* **2012,** *101*, (9), 2996-3018.
152. Cardew, P. T.; Davey, R. J. The kinetics of solvent-mediated phase transformations. *Proc. R. Soc. London, Ser. A* **1985,** *398*, (1815), 415-428.
153. Aaltonen, J.; Rades, T. Towards physico-relevant dissolution testing: The importance of solid-state analysis in dissolution. *Dissolution Technologies* **2009,** *16*.
154. Guzmán, H. R.; Tawa, M.; Zhang, Z.; Ratanabanangkoon, P.; Shaw, P.; Gardner, C. R.; Chen, H.; Moreau, J.-P.; Almarsson, Ö.; Remenar, J. F. Combined use of crystalline salt forms and precipitation inhibitors to improve oral absorption of celecoxib from solid oral formulations. *J. Pharm. Sci.* **2007,** *96*, (10), 2686-2702.

155. Surwase, S. A.; Itkonen, L.; Aaltonen, J.; Saville, D.; Rades, T.; Peltonen, L.; Strachan, C. J. Polymer incorporation method affects the physical stability of amorphous indomethacin in aqueous suspension. *Eur. J. Pharm. Biopharm.* **2015,** *96*, 32-43.
156. Warren, D. B.; Benameur, H.; Porter, C. J. H.; Pouton, C. W. Using polymeric precipitation inhibitors to improve the absorption of poorly water-soluble drugs: A mechanistic basis for utility. *J. Drug Target.* **2010,** *18*, (10), 704-731.
157. European Pharmacopoeia 9.5. European Directorate for the Quality of Medicines & HealthCare.
158. Aaltonen, J.; Heinänen, P.; Peltonen, L.; Kortejärvi, H.; Tanninen, V. P.; Christiansen, L.; Hirvonen, J.; Yliruusi, J.; Rantanen, J. In situ measurement of solvent-mediated phase transformations during dissolution testing. *J. Pharm. Sci.* **2006,** *95*, (12), 2730-2737.
159. Kaneniwa, N.; Otsuka, M.; Hayashi, T. Physicochemical characterization of indomethacin polymorphs and the transformation kinetics in ethanol. *Chem. Pharm. Bull. (Tokyo)* **1985,** *33*, (8), 3447-3455.
160. Koranne, S.; Thakral, S.; Suryanarayanan, R. Effect of formulation and process parameters on the disproportionation of indomethacin sodium in buffered lyophilized formulations. *Pharm. Res.* **2018,** *35*, (1).
161. Crowley, K. J.; Zografi, G. Cryogenic grinding of indomethacin polymorphs and solvates: Assessment of amorphous phase formation and amorphous phase physical stability. *J. Pharm. Sci.* **2002,** *91*, (2), 492-507.
162. Peltonen, L.; Liljeroth, P.; Heikkilä, T.; Kontturi, K.; Hirvonen, J. Dissolution testing of acetylsalicylic acid by a channel flow method—correlation to USP basket and intrinsic dissolution methods. *Eur. J. Pharm. Sci.* **2003,** *19*, (5), 395-401.
163. Pan, Q.; Guo, P.; Duan, J.; Cheng, Q.; Li, H. Comparative crystal structure determination of griseofulvin: Powder X-ray diffraction versus single-crystal X-ray diffraction. *Chin. Sci. Bull.* **2012,** *57*, (30), 3867-3871.
164. Cheng, K. C.; Shefter, E.; Srikrishnan, T. Crystal structure analysis of the desolvation of the chloroform solvate of griseofulvin. *Int. J. Pharm.* **1979,** *2*, (2), 81-89.
165. Cox, P. J.; Manson, P. L. [gamma]-indomethacin at 120 K. *Acta Crystallogr. Sect. Sect. E: Struct. Rep. Online* **2003,** *59*, (7), o986-o988.
166. Chen, X.; Morris, K. R.; Griesser, U. J.; Byrn, S. R.; Stowell, J. G. Reactivity differences of indomethacin solid forms with ammonia gas. *J. Am. Chem. Soc.* **2002,** *124*, (50), 15012-15019.
167. Zhu, Q.; Harris, M. T.; Taylor, L. S. Modification of crystallization behavior in drug/polyethylene glycol solid dispersions. *Mol. Pharm.* **2012,** *9*, (3), 546-553.
168. Mosén, K.; Bäckström, K.; Thalberg, K.; Schaefer, T.; Axelsson, A.; Kristensen, H. G. The apparent plasticizing effect of polyethylene glycol (PEG) on the crystallinity of spray dried lactose/PEG composites. *Eur. J. Pharm. Biopharm.* **2006,** *64*, (2), 206-211.
169. Friesen, D. T.; Shanker, R.; Crew, M.; Smithey, D. T.; Curatolo, W. J.; Nightingale, J. A. S. Hydroxypropyl methylcellulose acetate succinate-based spray-dried dispersions: An overview. *Mol. Pharm.* **2008,** *5*, (6), 1003-1019.
170. Zhang, S.-W.; Yu, L.; Huang, J.; Hussain, M. A.; Derdour, L.; Qian, F.; de Villiers, M. M. A method to evaluate the effect of contact with excipients on the surface crystallization of amorphous drugs. *AAPS PharmSciTech* **2014,** *15*, (6), 1516-1526.
171. Tres, F.; Treacher, K.; Booth, J.; Hughes, L. P.; Wren, S. A. C.; Aylott, J. W.; Burley, J. C. Indomethacin-Kollidon VA64 extrudates: A mechanistic study of pH-dependent controlled release. *Mol. Pharm.* **2016,** *13*, (3), 1166-1175.

ISBN 978-951-51-5738-6 (PRINT)
ISBN 978-951-51-5739-3 (ONLINE)
ISSN 2342-3161 (PRINT)
ISSN 2342-317X (ONLINE)
http://ethesis.helsinki.fi

HELSINKI 2020